Report No. KS-24-05 ▪ FINAL REPORT ▪ September 2024

Low-Shrinkage Ultra-High-Performance Concrete

Yasmeen Aljawad
Rémy D. Lequesne, Ph.D., P.E.
Matt O'Reilly, Ph.D., P.E.

The University of Kansas

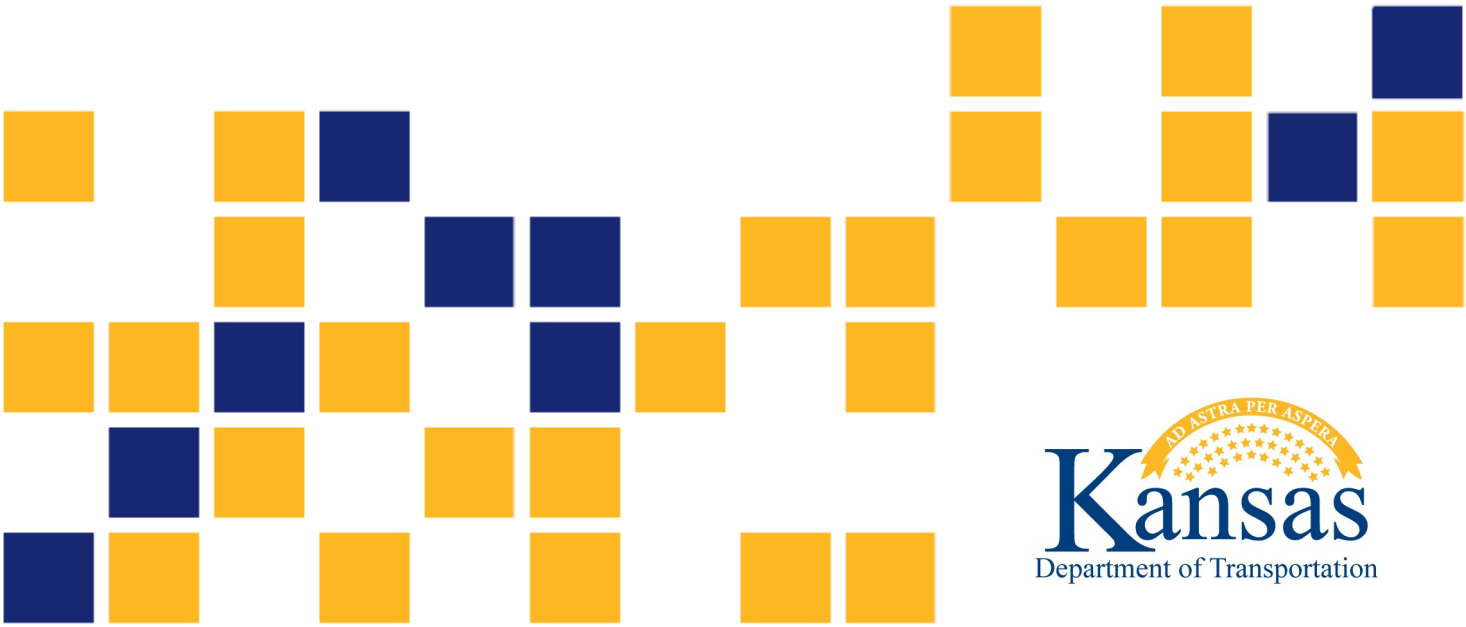

Kansas Department of Transportation

1 Report No. KS-24-05	**2 Government Accession No.**	**3 Recipient Catalog No.**
4 Title and Subtitle Low-Shrinkage Ultra-High-Performance Concrete		**5 Report Date** September 2024 **6 Performing Organization Code**
7 Author(s) Yasmeen Aljawad Rémy D. Lequesne, Ph.D., P.E. Matt O'Reilly, Ph.D., P.E.		**8 Performing Organization Report No.**
9 Performing Organization Name and Address The University of Kansas Department of Civil, Environmental & Architectural Engineering 1530 West 15th St Lawrence, Kansas 66045-7609		**10 Work Unit No. (TRAIS)** **11 Contract or Grant No.** C2177
12 Sponsoring Agency Name and Address Kansas Department of Transportation Bureau of Research 2300 SW Van Buren Topeka, Kansas 66611-1195		**13 Type of Report and Period Covered** Final Report January 2021–June 2022 **14 Sponsoring Agency Code** RE-0827-01
15 Supplementary Notes For more information write to address in block 9.		

16 Abstract

Ultra-high-performance concrete (UHPC) has been used increasingly in the past decade due to its high strength, rapid strength gain, and enhanced durability. UHPC is a cement-based material that typically has a low w/cm ratio, high paste content, and a 2% volume fraction of 0.5-in. long, straight, high-strength steel fibers. Most commercially available UHPC mixtures are also proprietary, or company-owned, which tends to elevate its cost. To lower the cost of UHPC in Kansas, this research aimed to develop non-proprietary UHPC using primarily Kansas-based materials. It was important that the proposed mixture gain strength quickly for use in accelerated bridge construction; the proposed mixture proportions have produced measured 1-, 7-, and 28-day compressive strengths as high as 13.1, 16.8, and 19.6 ksi. Also, because UHPC typically exhibits high early-age shrinkage relative to conventional concrete, this research explores shrinkage-limiting methods, including a shrinkage reducing admixture (SRA), a shrinkage compensating admixture (SCA), and prewetted lightweight aggregates (LWAs). The SRA effectively reduced UHPC shrinkage by one-third 30 to 60 days after mixing, but not at 90 days. The SCA reduced shrinkage throughout the 90 days of monitoring, and the effect was highly dose dependent. LWA did not reduce UHPC shrinkage in this study, but further research is needed since this finding conflicts with prior research. Results are also reported from tension and bending tests of UHPC with different volume fractions of high-strength straight and hooked steel fibers. Every specimen tested exhibited strain hardening in tension or deflection hardening in bending, suggesting that both fiber types are similarly effective. However, further research is needed to conclusively compare fibers due to the scope of the reported tests.

17 Key Words Ultra High Performance Concrete, Durability, Lightweight Aggregates, Steel Fibers		**18 Distribution Statement** No restrictions. This document is available to the public through the National Technical Information Service www.ntis.gov.	
19 Security Classification (of this report) Unclassified	**20 Security Classification (of this page)** Unclassified	**21 No. of pages** 71	**22 Price**

Form DOT F 1700.7 (8-72)

This page intentionally left blank.

LOW-SHRINKAGE ULTRA-HIGH-PERFORMANCE CONCRETE

Final Report

Prepared by:

Yasmeen Aljawad

Rémy D. Lequesne, Ph.D., P.E.

Matt O'Reilly, Ph.D., P.E.

The University of Kansas

A Report on Research Sponsored by:

THE KANSAS DEPARTMENT OF TRANSPORTATION

TOPEKA, KANSAS

and

THE UNIVERSITY OF KANSAS

LAWRENCE, KANSAS

September 2024

NOTICE

The authors and the state of Kansas do not endorse products or manufacturers. Trade and manufacturers names appear herein solely because they are considered essential to the object of this report.

This information is available in alternative accessible formats. To obtain an alternative format, contact the Office of Public Affairs, Kansas Department of Transportation, 700 SW Harrison, 2nd Floor – West Wing, Topeka, Kansas 66603-3745 or phone (785) 296-3585 (Voice) (TDD).

DISCLAIMER

The contents of this report reflect the views of the authors who are responsible for the facts and accuracy of the data presented herein. The contents do not necessarily reflect the views or the policies of the state of Kansas. This report does not constitute a standard, specification or regulation.

Abstract

Ultra-high-performance concrete (UHPC) has been used increasingly in the past decade due to its high strength, rapid strength gain, and enhanced durability. UHPC is a cement-based material that typically has a low *w/cm* ratio, high paste content, and a 2% volume fraction of 0.5-in. long, straight, high-strength steel fibers. Most commercially available UHPC mixtures are also proprietary, or company-owned, which tends to elevate its cost. To lower the cost of UHPC in Kansas, this research aimed to develop non-proprietary UHPC using primarily Kansas-based materials. It was important that the proposed mixture gain strength quickly for use in accelerated bridge construction; the proposed mixture proportions have produced measured 1-, 7-, and 28-day compressive strengths as high as 13.1, 16.8, and 19.6 ksi. Also, because UHPC typically exhibits high early-age shrinkage relative to conventional concrete, this research explores shrinkage-limiting methods, including a shrinkage reducing admixture (SRA), a shrinkage compensating admixture (SCA), and prewetted lightweight aggregates (LWAs). The SRA effectively reduced UHPC shrinkage by one-third 30 to 60 days after mixing, but not at 90 days. The SCA reduced shrinkage throughout the 90 days of monitoring, and the effect was highly dose dependent. LWA did not reduce UHPC shrinkage in this study, but further research is needed since this finding conflicts with prior research. Results are also reported from tension and bending tests of UHPC with different volume fractions of high-strength straight and hooked steel fibers. Every specimen tested exhibited strain hardening in tension or deflection hardening in bending, suggesting that both fiber types are similarly effective. However, further research is needed to conclusively compare fibers due to the scope of the reported tests.

Acknowledgments

Funding for this study was provided by the Kansas Department of Transportation. Material support was provided by Bekaert, Euclid Chemical, Midwest Concrete Materials, Monarch Cement Company, and Norchem Corp.

Table of Contents

List of Figures

List of Tables

Chapter 1: Introduction

1.1 Motivation

Ultra-high-performance concrete (UHPC) has become increasingly common due to its high strength, rapid strength gain, and considerable durability compared to conventional concrete. These attributes make UHPC desirable for many applications, including in accelerated bridge construction. However, the high cost of UHPC – due in part to the prevalence of proprietary mixtures – has slowed its implementation. Therefore, a primary aim of the current work was to reduce UHPC costs in Kansas by developing a non-proprietary UHPC mixture design using primarily Kansas-based materials. Because the intended application is primarily in joints (pour strips) between precast members in accelerated bridge construction projects, higher priority was placed on rapid strength gain than on high ultimate strength.

UHPC uses high contents of cementitious materials and a low water-to-cementitious materials (*w/cm*) ratio to achieve its high strength, but these properties also cause it to exhibit more early-age shrinkage than conventional concrete. When UHPC is used for joints between precast members, excessive shrinkage might cause the UHPC to pull away from the precast concrete, exposing the reinforcing bars crossing the joint to moisture, oxygen, and road salts. Consequently, the effectiveness of shrinkage-limiting methods in UHPC must be investigated. This research explored the efficacy of shrinkage reducing admixtures (SRAs), shrinkage compensating admixtures (SCAs), and prewetted lightweight aggregates (LWAs) for internal curing, which all tend to reduce shrinkage of conventional concrete.

1.2 Scope of Work

The aim of this research was to develop a non-proprietary low-shrinkage ultra-high-performance concrete using Kansas-based materials. The main goal was to design a UHPC mixture design that rapidly gains strength to allow minimum construction time. This study also explored the effectiveness of SRAs, SCAs, and LWAs. Research results from 22 batches of concrete are reported. The first eight batches were done to achieve a slump flow of 27 inches and a seven-day strength of 14 ksi, similar to UHPC in Yuan and Graybeal (2014). Subsequent batches were done to experiment with shrinkage-limiting methods and various types and volume fractions of fibers.

Chapter 2: Literature Review

2.1 Introduction to Ultra-High-Performance Concrete

UHPC is a relatively new cement-based material that exhibits a high compressive strength, high tensile strength, and low permeability that enhances durability. Although high-strength concrete can be brittle, the use of high-strength steel fibers causes UHPC to exhibit considerable ductility in both tension and compression. UHPC typically requires a high content of cementitious materials, which causes it to exhibit considerable early-age shrinkage due to a high heat of hydration, high paste content, and low water-to-binder ratio (Liu et al., 2017).

In the United States, UHPC is primarily used in applications related to the highway system, specifically in I-girders and bridge superstructures and most often in pour-strips between precast girders and other types of joints in accelerated bridge construction (Graybeal, 2008). Although related code provisions are lacking, the enhanced mechanical properties of UHPC, such as high early strength that reduces construction time, have made it desirable to many state departments of transportation, including the Kansas Department of Transportation (KDOT).

2.2 Non-Proprietary Ultra-High-Performance Concrete

The high compressive strength of UHPC is achieved in part by having a low water-to-cementitious materials (*w/cm*) ratio, typically below 0.22. It is also common to use silica fume in UHPC, which contributes to the strength of UHPC by converting the lime in portland cement concrete to additional calcium silicate hydrate (C-S-H) (Magureanu et al., 2012). Due to its small particle size, silica fume also fills voids in the concrete and improves the homogeneity of the mixture. This homogeneity, which is also achieved through selection of well-graded fine aggregates, is another important factor that contributes to the high compressive strength of UHPC.

The tensile strength and ductility of UHPC are directly related to the type and volume fraction of fibers, and the fiber volume fraction required in UHPC depends on the strength and length-to-diameter ratio of the fibers themselves (Wille & Boisvert-Cotulio, 2015; Alkaysi & El-Tawil, 2016). Yuan and Graybeal (2015) used a 2% volume fraction of straight steel fibers and obtained acceptable mechanical properties. Larger volume fractions increase the cost of UHPC, reduce its workability, and have diminishing benefits in terms of tensile strength and compression

deformation capacity. Use of large quantities of fibers has only marginal effects on compressive strength (Alsalman et al., 2020).

High-range water reducers (HRWRs) and other admixtures are necessary for UHPC to achieve acceptable workability. HRWRs are typically selected based on availability, effectiveness, compatibility with other mixture constituents, and cost. Although there are no specified material properties for the selection of HRWR, the effective interaction of HRWR with the cement paste is important for UHPC workability and strength (Wille & Boisvert-Cotulio, 2015). Different types of HRWR may interact uniquely with a given mixture, so trial batches are necessary to select dosages. Overuse of HRWR can negatively impact the compressive strength of UHPC and tends to add entrained air, which increases the porosity of the material (Alsalman et al., 2020).

Although proprietary UHPC mixtures have been available for many years, various research groups have recently developed non-proprietary UHPC mixtures. Wille et al. (2011a, 2011b) proposed several non-proprietary UHPC mixture designs that can exceed a compressive strength of 22 ksi without special curing procedures. Wille and Boisvert-Cotulio (2015) investigated the specific qualities of various constituent materials needed to obtain the mechanical properties of UHPC while remaining cost effective and also proposed UHPC mixture designs. Each of their recommended mixture designs used materials selected from specific regions of the United States. Table 2.1 lists the mixture designs proposed by Wille and Boisvert-Cotulio (2015) for materials from the upper-midwestern United States, which is the region in their study nearest to Kansas.

Table 2.1: Mixture Proportions Proposed by Wille and Boisvert-Cotulio (2015)

Materials	Mixture Design 1 (lb/yd^3)	Mixture Design 2 (lb/yd^3)
Cement	1269	1278
Silica fume	317	320
Fly ash	308	310
Fine aggregate	1903	-
Fine + coarse aggregates	-	1918
High-range water reducer	46	46
w/cm	0.24	0.22

Subsequently, other researchers have also developed non-proprietary UHPC mixture designs (Alkaysi & El-Tawil, 2016; Aghdasi, Heid, & Chao, 2016; Meng, Valipour, Khayat, 2016; Castine, 2017; and Floyd et al., 2020). Table 2.2 lists mixture proportions recommended by Floyd et al. (2020).

Table 2.2: Mixture Proportions Proposed by Floyd et al. (2020)

Materials	Mixture Design (lb/yd^3)
Cement	1180
Silica fume	197
Slag	590
Fine masonry sand	1966
Fibers	255
High-range water reducer	16 (oz/cwt)
w/cm	0.20

Using previous research on non-proprietary UHPC as a starting point, non-proprietary UHPC mixture designs need to be developed using Kansas-based materials to facilitate the use of UHPC in Kansas-specific applications.

2.3 Concrete Shrinkage

ACI 209.1R-05 defines concrete shrinkage as "the decrease in either length or volume of a material resulting from changes in moisture content or chemical changes." ACI 209.1R-05 and Mindess, Young, and Darwin (2003) provide in-depth explanations of the factors affecting the shrinkage and creep of hardened concrete. UHPC tends to exhibit substantially more shrinkage than conventional concrete due to its high paste content and low *w/cm* ratio (Čítek, Rydval, & Kolísko, 2016). This may not be a concern in some UHPC applications because its high strength tends to reduce or prevent development of shrinkage cracks. However, when UHPC is used for joint strips, the high shrinkage can potentially cause the UHPC to separate from the adjoining precast concrete and expose reinforcing bars crossing the joint. This potential opening would put the reinforcing bars at risk of corroding. Therefore, research is needed to explore ways to limit UHPC shrinkage.

Common methods for limiting the shrinkage of hardened concrete include the use of shrinkage reducing admixtures (SRAs), shrinkage compensating admixtures (SCAs), and internal curing. Internal curing methods include the use of prewetted lightweight aggregates (LWAs), superabsorbent polymers (SAPs), bentonite clay, shale pottery, or cellulose fibers (Liu et al., 2017). The effectiveness of SRAs, SCAs, and internal curing with LWA in conventional concrete, high-performance concrete, and UHPC are discussed in the following section.

2.3.1 Conventional Concrete and High-Performance Concrete

SRAs function by reducing the surface tension of the pore fluid, which then reduces concrete shrinkage. Some research has indicated that using SRAs can reduce the shrinkage up to 50% relative to a control mixture (Feng & Darwin, 2020).

SCAs cause concrete swelling that offset shrinkage strains. Chen and Brouwers (2012) concluded that SCAs can effectively offset shrinkage, and that considerable expansion only occurs with 10% of SCA or greater. They also observed a slower compressive strength gain in concrete specimens with 15% of SCA or greater.

Prior research has shown that the use of LWAs for internal curing effectively reduces the early-age shrinkage of conventional concrete and low-cracking high-performance concrete (LC-HPC). Feng and Darwin (2020) found that internal curing effectively reduced the shrinkage of LC-HPC; furthermore, the use of internal curing resulted in a greater percentage of total shrinkage occurring at later ages, when the concrete had gained more strength and would be less prone to cracking. Pendergrass and Darwin (2014) and Pendergrass et al. (2017) researched the effectiveness of combining LWA, slag, and silica fume on reducing concrete shrinkage. They found that, although prewetted LWA effectively reduced concrete shrinkage, the combination of LWA, slag, and silica fume further reduced the early-age (up to 30 days) and the long-term (up to 365 days) concrete shrinkage. Deboodt, Fu, and Ideker, (2016) also found that the combination of pre-wetted LWA and SRA effectively reduced autogenous shrinkage.

2.3.2 Ultra-High-Performance Concrete

Similar to conventional concrete, SRAs reduce UHPC shrinkage caused by capillary tension by decreasing the surface tension (Xie et al., 2018). SRAs also delay the hardening of the

cement paste, which tends to reduce the autogenous and chemical shrinkage of UHPC (Xie et al., 2018).

The authors are not aware of prior work done regarding the use of SCAs to limit UHPC shrinkage, although related work has used expanding agents (EAs) to limit shrinkage (Li et al., 2017; Teng, Valipour, & Khayat, 2021). Use of EAs alone (without LWAs) reduced the mechanical properties of UHPC but effectively caused expansion (Li et al., 2017).

The low *w/cm* ratio in UHPC can cause the cement particles to have a low degree of hydration, typically less than 50%, as less free water is available to the cement than in conventional concrete. This low degree of hydration contributes to early-age shrinkage by increasing the capillary tension of pore fluid (Justs et al., 2015), a process known as autogenous shrinkage. Internal curing using LWAs or other means has been shown to effectively reduce autogenous shrinkage of UHPC because internal curing releases water stored in the pores of an absorbent material to the concrete over time, allowing for more complete cement hydration (Liu et al., 2017). Justs et al. (2015) concluded that the addition of superabsorbent polymers reduced shrinkage with a dosage of 20% or higher but also reduced the mechanical properties of UHPC. Meng and Khayat (2017) also investigated the effectiveness of prewetted LWAs for internal curing in UHPC and found that UHPC showed a 60% reduction in early-age shrinkage with up to 75% prewetted LWA.

Research has also shown the benefits of combining SRAs or expansive agents with LWAs. Li et al. (2017) found that combining expansive agents and prewetted LWA effectively reduced UHPC shrinkage because internal curing compensates for moisture loss during hydration and drying and the expansive agents compensate for shrinkage without compromising the mechanical properties of UHPC. They also found that internal curing with LWA increased the compressive strength of UHPC, in contrast to the findings of Justs et al. (2015), in which the researchers used SAPs and not LWA.

Despite the previous findings, additional study of SRAs, SCAs, and LWAs in UHPC is needed because (1) only a limited number of studies have investigated shrinkage-reduction strategies in UHPC, and (2) conflicting findings of shrinkage reduction effectiveness and the effects on the mechanical properties of UHPC have been reported.

Chapter 3: Experimental Work

The first portion of this research focused on the development of a non-proprietary UHPC mixture design using constituent materials readily available in Kansas and a targeted compressive strength of 14 ksi within seven days of mixing. Mixture designs published by Wille and Boisvert-Cotulio (2015) were used as a starting point and then modified to achieve the desired results for early-age strength. The second portion of this research focused on strategies for reducing UHPC shrinkage, including SRAs, SCAs, and LWAs. The effectiveness of these technologies for limiting UHPC shrinkage is reported. A small number of tests were also conducted to document the behavior of the resulting UHPC in compression, tension, and bending.

3.1 Materials

Table 3.1 lists the materials used in this study, their source, attributes, and the reason for selecting each material. Locally sourced materials were preferred.

A high content of $C_2S + C_3S$ in cement is important for strength gain in concrete. It also indicates a low content of C_4AF, which can impact the set time of the concrete negatively and cause it to set too quickly. A Blaine Fineness of 400 m^2/kg is common in Type I cement and helps obtain the necessary mixture homogeneity (Wille & Boisvert-Cotulio, 2015).

Previous research has shown that a silica fume with a very low carbon content and small particle size contributes to relatively low water demand and a higher packing density at small dosages (Wille & Boisvert-Cotulio, 2015). These are important for UHPC since high strength requires a very low *w/cm* ratio (0.2 or lower). In this study, Class C fly ash was selected because it tends to increase the early-age concrete compressive strength, a critical property for the intended application (closure strips in bridge decks). Class F fly ash tends to increase long-term compressive strength and was therefore less ideal for this application.

Table 3.1: Material Properties

Material	Source	Product Name	ASTM Standard	Attributes	Reasoning
Cement	Monarch Cement Company	Type I portland cement	ASTM C150	Specific Gravity = 3.13 Loss on ignition = 1.46% Blaine fineness = 459.8 m^2/kg $C_2S + C_3S$ content = 68.1% C4AF content = 9%	Low C_4AF content ($1\% \leq C_4AF \leq 11\%$)[1] Minimum Blaine fineness of 400 m^2/kg[1] High $C_2S + C_3S$ content ($65\% \leq C_2S + C_3S \leq 87\%$)[1]
Silica fume	Norchem	Silica fume	ASTM C1240	SiO2 content = 90%	High SiO_2 content ($85\% \leq SiO_2 \leq 95\%$)[1] Low carbon content ($0.30\% \leq$ carbon $\leq 0.70\%$)[1]
Fly ash	Ash Grove	Class C fly ash	ASTM C618	SiO2 = 41.75% Fe2O3 = 5.51% Al2O3 = 18.04% CaO = 24.02% Blaine fineness = 28.3 Loss on ignition = 0.33%	Class C fly ash selected to increase early-age strength

Material	Source	Product Name	ASTM Standard	Attributes	Reasoning
Pea gravel	Midwest Concrete Materials	Pea gravel	ASTM C33	Specific gravity = 2.60 Fineness modulus = 4.91	Based on availability and gradation (Figure 3.1)
Sand	Midwest Concrete Materials	Kansas river sand	ASTM C33	Specific gravity = 2.61 Fineness modulus = 3.03	Based on availability and gradation (Figure 3.2)
Lightweight aggregate	Buildex	Expanded shale	ASTM C33	Specific gravity = 1.67 Fineness modulus = 4.45	Based on availability and gradation (Figure 3.3)
High range water reducer (HRWR)	Euclid Chemicals	Plastol 6400 EXT	ASTM C494 (Type F)	-	Recommended by supplier
Shrinkage compensating admixtures (SCAs)	Euclid Chemicals	Conex	ASTM C494 (Type S)	-	Compatibility with HRWR
Shrinkage reducing admixtures (SRAs)	Euclid Chemicals	Eucon SRA XT	ASTM C494 (Type S)	-	Compatibility with HRWR
Straight fiber 1	HiPer Fiber	Type A Straight Steel Fibers	ASTM A820	0.008 in. diameter 0.5 in. length Tensile strength $\geq$ 413 ksi	Commonly used in UHPC
Straight fiber 2	Nycon	SF Type I-N	ASTM A820	0.008 in. diameter 0.5 in. length Tensile strength $\geq$ 285 ksi	Commonly used in UHPC
Hooked fiber	Bekaert	Dramix RC-80/30-BP	ASTM A820	0.015 in. diameter 1.18 in. length Tensile strength $\geq$ 445 ksi	For comparison with straight fibers

[1] Recommended by Wille and Boisvert-Cotulio (2015).

Figures 3.1 to 3.3 show the particle size distribution of pea gravel, river sand, and LWA. The selection process included identifying materials that would complement each other in terms of particle size to obtain a mixture design that was well-graded across all constituent materials. Because the desired compressive strength of UHPC requires well-graded materials to minimize voids in the mixture, the pea gravel gradation was not ideal. However, as shown in Figure 3.2, it was used in limited quantities as a complement to well-graded sand to obtain an overall well-graded combination of aggregates.

Most batches with fibers had either Straight Fiber 1 or Straight Fiber 2, which were used interchangeably in this study. These fibers had the same nominal geometry and were similar to the straight fibers commonly used in UHPC mixtures. The difference in tensile strengths between these fibers had no effect on the study results because the fibers pulled out and did not fracture during testing. A small number of batches were done using a hooked fiber (Dramix RC-80/30-BP fiber), which might be an effective alternative to the common straight fibers for UHPC mixtures.

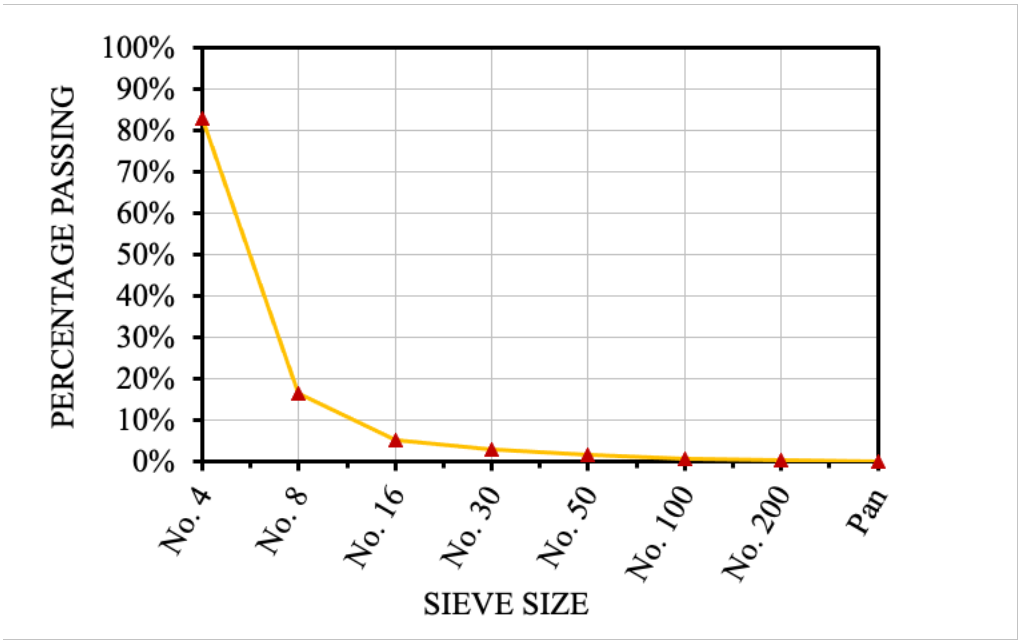

Figure 3.1: Particle Size Distribution for Pea Gravel

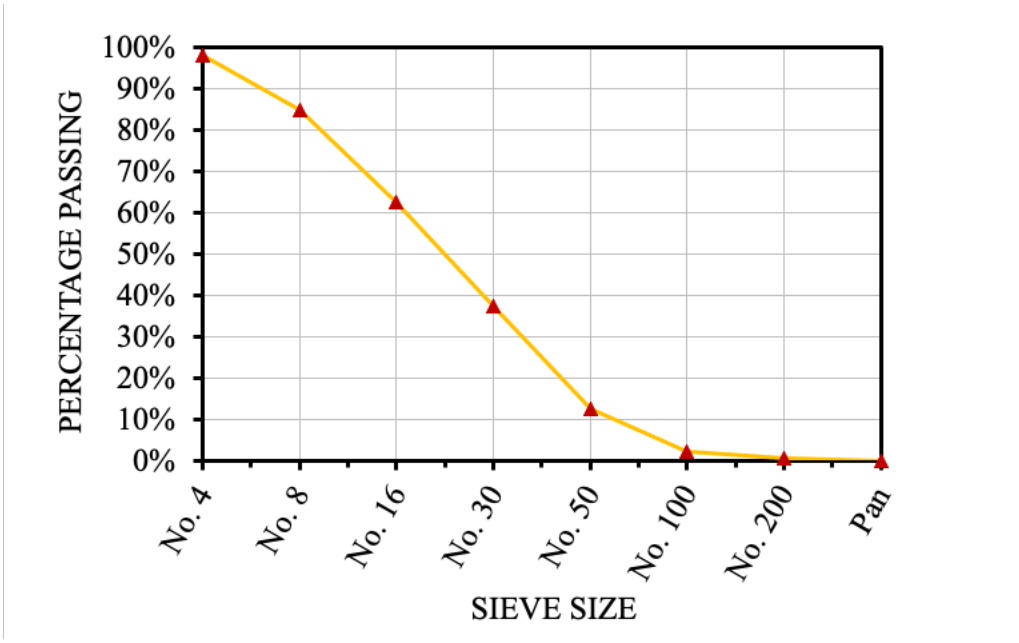

Figure 3.2: Particle Size Distribution for River Sand

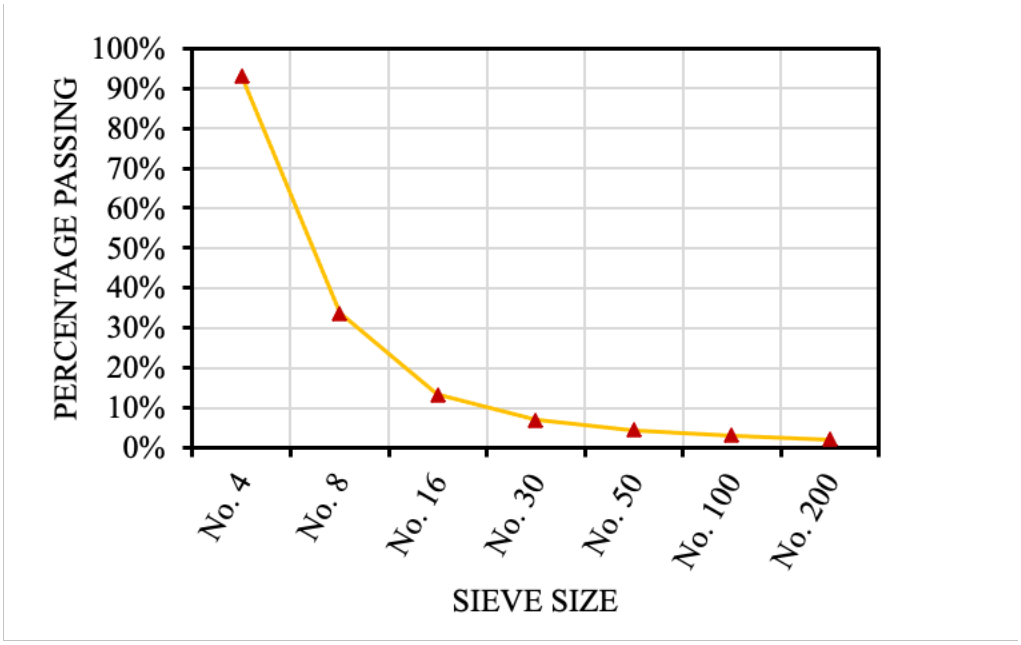

Figure 3.3: Particle Size Distribution for LWA

3.2 Mixture Proportions

Twenty-eight batches were made with varied mixture proportions and constituents. Batches prior to Batch B1–FlyAsh were trial batches and are not reported herein. Tables 3.2 and

3.3 provide information on the 22 batches addressed in this report (mixture proportions are provided in Appendix A). Batches B1–FlyAsh to B6 did not include fibers and were done to refine the mixture proportions to obtain the desired concrete compressive strength and workability. Batches B2–PeaGravel and B3–PeaGravel were the only two batches that included pea gravel. Although coarse aggregate is beneficial because it reduces cost, pea gravel was shown to decrease compressive strength in this study and was omitted from later batches.

After the desired early-age strength was achieved with Batch B6, 2% by volume of straight fibers was added to each batch starting with Batch B7–Fibers2%. The mixture proportions were modified slightly to improve the workability in Batch B8–Baseline, resulting in the desired workability and strength, making it the baseline mixture design for subsequent batches. Table 3.2 shows the mixture proportions for Batch B8–Baseline, the baseline mixture design. Subsequent batches were variations of Batch B8–Baseline to investigate the utility of shrinkage-reducing technologies in UHPC. Table 3.3 shows how the mixture proportions of each of the other 21 batches differed from the baseline mixture design.

Batches B9–SCA2% to B16–LWA30% were used to experiment with admixtures aimed at limiting UHPC shrinkage. Three batches were mixed with SRAs and three more with SCAs. Dosages for these batches were selected to be near the low, middle, and high ends of the manufacturer-recommended dosage ranges. Batches B15–LWA15% and B16–LWA30% included different dosages of LWA to experiment with internal curing and observe its effect on shrinkage of concrete; both dosage selections were based on prior research (Lafikes, Darwin, & O'Reilly, 2020). Batches B17 to B22–3%HF had different fiber types and volume fractions.

Table 3.2: Baseline Mixture Proportions

Material	lb per yd^3
Cement	1362
Silica Fume	274
Fine Aggregate	1909
Water	312
HRWR	26.0
Fibers	265
w/cm	0.20

Table 3.3: Mixture Constituents

Batch I.D.	Main Variables
B1–FlyAsh	*w/cm* = 0.22, fly ash, HRWR (18.9 oz/cwt), no fibers
B2–PeaGravel	*w/cm* = 0.22, fly ash, coarse aggregate, HRWR (17.8 oz/cwt), no fibers
B3–PeaGravel	*w/cm* = 0.22, fly ash, coarse aggregate, HRWR (18.2 oz/cwt), no fibers
B4–FlyAsh	*w/cm* = 0.20, fly ash, HRWR (18.2 oz/cwt), no fibers
B5–FlyAsh	*w/cm* = 0.20, fly ash, HRWR (24.6 oz/cwt), no fibers
B6	*w/cm* = 0.20, HRWR (20.7 oz/cwt), no fibers
B7–Fibers2%	*w/cm* = 0.20, HRWR (22.1 oz/cwt)
B8–Baseline	Baseline mixture[1]
B9–SCA2%	*w/cm* = 0.20, HRWR (23.3 oz/cwt), SCA 2%[2] by weight of cementitious
B10–SCA6%	*w/cm* = 0.20, HRWR (24.8 oz/cwt), SCA 6% by weight of cementitious
B11–SCA10%	*w/cm* = 0.20, HRWR (30.1 oz/cwt), SCA 10%[2] by weight of cementitious
B12-SRA0.5%	*w/cm* = 0.20, HRWR (24.9 oz/cwt), SRA 0.5%[2] by weight of cementitious
B13–SRA1.25%	*w/cm* = 0.20, HRWR (24.8 oz/cwt), SRA 1.25% by weight of cementitious
B14–SRA2%	*w/cm* = 0.20, HRWR (26.1 oz/cwt), SRA 2%[2] by weight of cementitious
B15–LWA15%	*w/cm* = 0.20, HRWR (25.8 oz/cwt), LWA 15% by weight of cementitious
B16–LWA30%	*w/cm* = 0.20, HRWR (24.1 oz/cwt), LWA 30% by weight of cementitious
B17	*w/cm* = 0.20, HRWR (48.4 oz/cwt)
B18–3%SF	*w/cm* = 0.20, HRWR (77.1 oz/cwt), 3% straight fibers by volume
B19–2%HF	*w/cm* = 0.20, HRWR (58.2 oz/cwt), 2% hooked fibers by volume
B20–2%HF	*w/cm* = 0.20, HRWR (56.2 oz/cwt), 2% hooked fibers by volume
B21–2%HF	*w/cm* = 0.20, HRWR (57.2 oz/cwt), 2% hooked fibers by volume
B22–3%HF	*w/cm* = 0.20, HRWR (49.3 oz/cwt), 3% hooked fibers by volume

[1] Refer to Table 3.2.

[2] Lower/upper limits of dosage rates recommended by Euclid Chemicals.

3.3 Mixing Procedures and Specimen Fabrication

Materials were weighed in separate buckets approximately 12 hours before mixing and covered with lids or towels to limit changes in moisture content. Forms were oiled and kept aside until the mixing process was complete. Except for Batches B17 and B18–3%SF, which were mixed

in a drum mixer, mixing was done using a counter-current pan mixer and not the high-shear mixers typically used for UHPC production.

In addition to using well-graded materials, previous research has shown that thorough mixing of dry materials is necessary to achieve a high particle-packing density (Wille & Boisvert-Cotulio, 2015). Therefore, this study practiced the following mixing procedure recommended by Wille and Boisvert-Cotulio (2015):

1. Mix all the sand and silica fume for five minutes.
2. Add cement to the mixer and mix for five minutes.
3. Add water and one-third of the HRWR and mix for five minutes.
4. Add the remaining HRWR and mix for five minutes.
5. Gradually add the fibers and mix for five minutes.

Figures 3.4 to 3.7 show the process of concrete mixing. Initially blending the dry materials tends to break down clumps in the sand and silica fume and allows for a more homogeneous mixture (Figure 3.4). Due to the low *w/cm* ratio, the paste looked very dry, even after adding water (Figure 3.5). Addition of an HRWR reduces clumping of cement particles, thereby freeing water to increase workability. As a result of this mechanism, the mixture became very workable a few minutes after the HRWR was added (Figure 3.6). The fibers were added during the last step in the mixing process, which tends to reduce the workability of the concrete (Figure 3.7).

The freshly mixed concrete was placed in a wheelbarrow and transported to the location where specimens were fabricated. Specimens were fabricated by scooping the concrete from the wheelbarrow into the molds in no specific order. None of the specimens were rodded or tapped with a mallet except for Batch B6, which had no fibers and required rodding due to poor workability.

Figure 3.4: Mixture after Adding Cement

Figure 3.5: Mixture after Adding Water

Figure 3.6: Mixture after Adding HRWR

Figure 3.7: Mixture after Adding Fibers

3.4 Tests

3.4.1 Fresh-State Concrete Properties

Fresh-state concrete properties were measured within 5 minutes of mixing completion, or approximately 20 minutes after water was added to the mixer. Fresh-state properties of Batch B8–Baseline were also measured 30 minutes later to assess whether transportation time to the field would affect UHPC workability.

Fresh-state concrete testing was done for every batch. Tests included measuring the temperature (ASTM C1064), slump flow (ASTM C1611), J-ring (ASTM C1621 with filling procedure B), and unit weight (ASTM C138). Rodding and tapping were excluded from all tests to avoid disturbing the fiber distribution in the mixture per ASTM C1856. Although ASTM C1856 prescribes using equipment with dimensions specific to UHPC, the standard equipment prescribed in ASTM C1611 and C1621 was used to accommodate the longer fibers used in Batches B19–2%HF to B22–3%HF.

3.4.2 Hardened Concrete Properties

Compressive strength was measured in accordance with ASTM C39 at 1, 3 or 4, 7, 14, and 28 days after mixing for most batches. For each batch, six to ten 4×8 in. cylinders were cast in plastic molds. Specimens were demolded 24 $\pm$ 1 hours after water was added to the mixture and kept in a wet curing room until the day of testing. For Batch W, stress-strain behavior was evaluated at 28 days using two cylinders and a non-contact motion-tracking (Optotrak) system to record deformations. Figure 3.8 shows the placement of the Optotrak markers on the cylinders. Strain was calculated based on the change in distance between the topmost and bottommost rows of markers, which encompassed the middle half of the cylinder height.

Free shrinkage was measured in accordance with ASTM C157. Three specimens (3×3×11.25 in. each) were cast for Batches B1–FlyAsh to B16–LWA30% (examples are shown in Figure 3.9). Specimens were demolded 24 ± 1 hours after water was added to the mixture. After demolding, the specimens were kept in a limewater tank for 30 minutes to regulate their temperatures and then the first measurement was taken before returning them to be cured in the saturated limewater tank for six days. Specimens were then kept in a drying room that met the

requirements of ASTM C157. The length of each specimen was measured twice per week until 28 days after mixing, and then once per week until 90 days after mixing. The length change of each specimen was compared to the first measurement taken the day after water was added to the mixture to calculate shrinkage.

Figure 3.8: Marker Placement on Cylinder

Figure 3.9: Free-Shrinkage Specimens

Tension tests were done using the test setup and specimen type described in Tameemi et al. (2016) and Tameemi and Lequesne (2015). As shown in Figure 3.10, three prisms (6×6×20 in. each) were cast in plywood molds for Batches B17 to B22–3%HF, with two No. 8 reinforcing bars placed end-to-end along the longitudinal axis of the prism, intersecting at the mid length of the prism. When fabricating the specimens, the molds were filled to the top with concrete, and the top was leveled off with a trowel. No rodding or tapping was performed to avoid disrupting the distribution of fibers. After all specimens were cast, they were covered with damp plastic sheets and kept at room temperature for 24 $\pm$ 1 hours after water was added to the mixture. Specimens were then demolded and kept in a wet curing room for 27 $\pm$ 1 days.

On the day of testing, a 0.75 in. deep notch was sawn around the perimeter of the prism at mid length to force a crack to form where the two discontinuous reinforcing bars met. The specimens were loaded in tension by gripping the visible ends of the bars, which extended 6 in. from each end of the prism. Specimens were tested using a 120-kip hydraulic testing machine using the loading rates shown in Table 3.4.

Table 3.4: Loading Rates for Tension Tests

Loading Zone	Loading Rate (in./min)
0 to 2000 lb	0.1
2000 to 3000 lb	0.05
3000 to 4000 lb	0.03
Load > 4000 lb	0.016

An Optotrak system was used to record the positions of 16 markers attached to two faces of the specimen during each test. Figure 3.10 shows the tension prism forms and Figure 3.11 illustrates the placement of the markers. Marker position data were used to calculate the crack width during testing. Crack widths reported in Chapter 4 represent the width at the centroid of the specimen calculated from surface measurements assuming that plane sections remain plane.

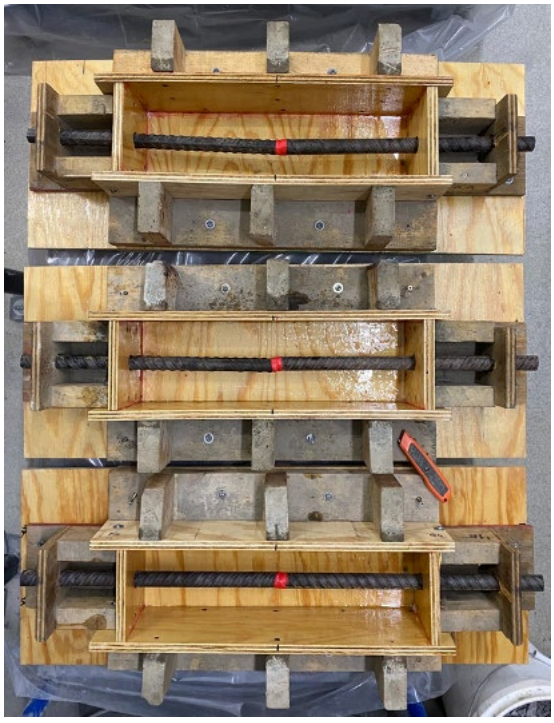

Figure 3.10: Tension Molds

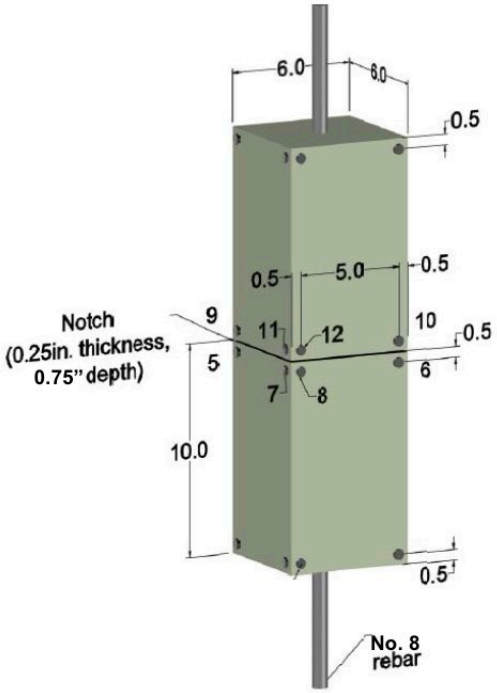

Figure 3.11: Tension Specimen
Source: Tameemi & Lequesne (2015)

Three beams (6×6×20 in. each) were cast in steel molds for Batches B17 to B22–3%HF. When fabricating the specimens, the molds were filled to the top with concrete and the top was leveled off with a trowel. No rodding or tapping was performed to avoid disrupting the fiber distribution. After all specimens were cast, they were covered with damp plastic sheets and kept at room temperature until 24 $\pm$ 1 hours after water was added to the mixture. Specimens were then demolded and kept in a wet curing room for 27 $\pm$ 1 days. The tests were performed using a 120-kip hydraulic testing machine in accordance with ASTM C1609, except that the loading rates in Table 3.5 were used. An Optotrak system was used to record the positions of eight markers (Figure 3.12). Beam deflection was calculated as the average vertical displacement of the markers at midspan minus the vertical displacement of the markers over the supports.

Table 3.5: Loading Rates for Beam Tests

Loading Zone	Loading Rate (in./min)
0 to 1000	0.10
1000 to 2000	0.05
2000 to 4000	0.01
Load > 4000	0.004

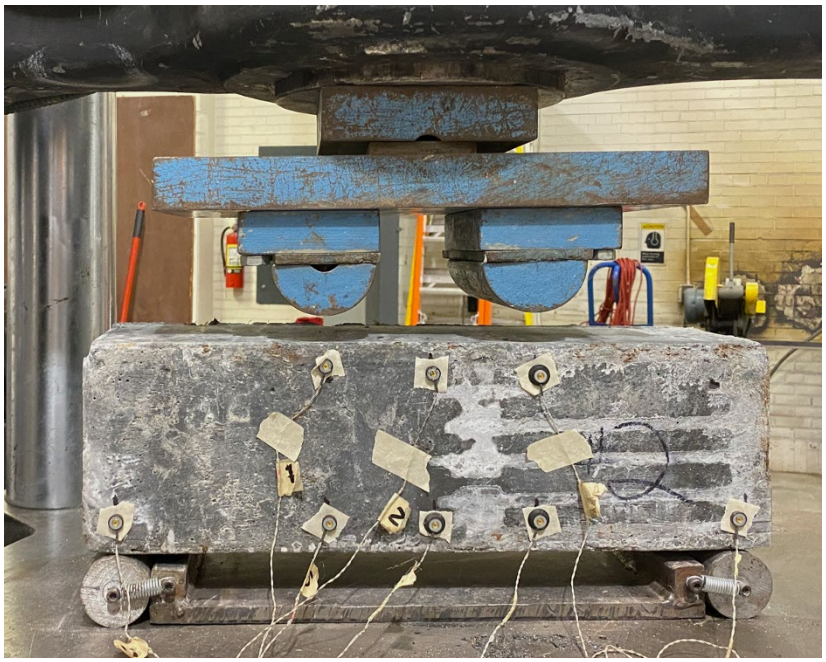

Figure 3.12: Beam Specimen with Eight Markers

3.5 Additional Tests

The Kansas Department of Transportation performed additional tests on the baseline mixture, including Volume of Permeable Voids (KT-73), Rapid Chloride Permeability (AASHTO T277), Surface Resistivity (KT-79), Hardened Air (ASTM C457), Freeze-Thaw (KTMR-22), and internal temperature over time. Results of these tests are documented in Appendix B.

Chapter 4: Test Results

4.1 Fresh-State Properties

Table 4.1 reports the fresh-state properties measured after mixing, including temperature, slump flow, J-ring, and unit weight. The fresh-state properties of Batch B8–Baseline were measured a second time, 30 minutes after mixing, to simulate the effects of transit time for UHPC mixed off-site. The batches had an average temperature of 78 °F, with a range of 68 to 86 °F. The lowest temperature was measured in Batch B13–SRA1.25% at 68 °F. The two highest temperatures were 86 °F and 82 °F in Batches B4–FlyAsh and B10–SCA6%, respectively. Both batches also had the lowest J-ring results at 15.5 in. and 16 in., respectively, which could be due to their high temperatures. The addition of steel fibers in Batches B7–Fibers2% to B22–3%HF resulted in increased unit weights, except for Batch B16–LWA30%, which had the lowest density (136.8 pcf) due to the high percentage of LWA. Table 4.1 also reports whether segregation was observed. For example, Batches B15–LWA15% and B16–LWA30%, which had LWA at a dosage of 15% and 30% of the weight of cementitious material, respectively, both exhibited segregation in the J-ring tests (Figures 4.1 and 4.2, respectively).

Figure 4.1: J-ring Test of Batch B15–LWA15%

Figure 4.2: J-ring Test of Batch B16–LWA30%, with clear evidence of segregation/blocking of the fibers at the inner perimeter of the J-ring

Although the HRWR dosage was increased in batches that included fibers, the slump flow and J-ring measurements for some batches with fibers were still notably less compared to those with no fibers. Batches B1–FlyAsh to B6 (without fibers) generally had a slump flow of more than 27 in., whereas Batches B7–Fibers2% to B22–3%HF, which all included fibers, generally had slump flow values in the range of 20 to 28 in. Batches B15–LWA15%, B16–LWA30%, and B17 were exceptions to this trend; these batches had slump flow values greater than 30 in. Batches B15–LWA15% and B16–LWA30% contained LWA, and Batch B17 had a high dosage of HRWR (48.4 oz cwt).

Table 4.1: Fresh-State Properties

Batch I.D.	Temp. (°F)	Slump Flow (in.)	J-ring (in.)	Blocking (Slump flow) - (J-ring) (in.)	Unit Wt. (pcf)	Segregation
B1–FlyAsh	69	28.25	26.00	2.25	146.6	No
B2–PeaGravel	72	27.0	25.50	1.50	144.4	No
B3–PeaGravel	72	37.75	-	-	143.6	No
B4–FlyAsh	86	15.5	14.75	0.75	142.8	No
B5–FlyAsh	70	27.75	20.75	7.00	144.0	No
B6	70	19.5	17.00	2.50	148.8	No
B7–Fibers2%	70	20.25	17.50	2.75	156.4	No
B8–Baseline	70	23.5	18.75	4.75	153.6	No
– [1]	-	23.0 [1]	19.50 [1]	3.50 [1]	-	No
B9–SCA2%	76	21.25	17.25	4.00	154.4	No
B10–SCA6%	82	22.0	16.00	6.00	156.0	No
B11–SCA10%	76	25.25	18.25	7.00	158.8	No
B12-SRA0.5%	74	24.0	18.75	5.25	159.2	No
B13–SRA1.25%	68	24.25	22.50	1.75	154.4	No
B14–SRA2%	72	28.0	28.00	0.00	153.2	No
B15–LWA15%	72	31.25	32.25	1.00	- [2]	Yes
B16–LWA30%	79	35.5	35.00	0.50	136.8	Yes
B17	80	33.25	30.50	2.75	154.4	Yes
B18–3%SF	77	26.25	23	3.25	152.8	Yes
B19–2%HF	74	24.75	17	7.75	154.7	Yes
B20–2%HF	75	24.75	19.5	5.25	155.3	Yes
B21–2%HF	77	24.25	16.75	7.5	158	Yes
B22–3%HF	74	23.75	17	6.75	159.3	Yes

[1] Properties were remeasured after 30 minutes to simulate transportation to a job site.
[2] Data collection error.

Blocking, which is the difference between the slump flow and J-ring test results, is also shown in Table 4.1. Blocking values in the table range from 0 to 7.75 in. Blocking values greater

than 2 in. are considered large (ASTM C1621). To assess whether adding fibers contributed to the large values, batches with no fibers, straight fibers, and hooked fibers were compared. A student's t-test was used to examine whether observed differences were statistically significant. A *p*-value > 0.05 indicated a difference that was not statistically significant, and a p-value $\leq$ 0.05 indicated a statistically significant difference. No statistically significant difference was observed between batches with straight fibers with an average blocking value of 2.75 in., and batches with no fibers, with an average of 3.25 in. (p = 0.692). There was, however, a statistically significant difference between batches with hooked fibers, with an average of 6.75 in., and batches with either no fibers or straight fibers (p = 0.020 and 0.007, respectively). In addition to fiber type, several other differences between the batches in Table 4.1 were observed, so further study is recommended.

4.2 Hardened-State Properties

4.2.1 Compressive Strength Gain

Table 4.2 summarizes the compressive strengths of Batches B1–FlyAsh to B22–3%HF at 1, 3 or 4, 7, 14, and 28 days. Each reported value is the average of one or two cylinders. Batches B1–FlyAsh to B5–FlyAsh, which included either fly ash or pea gravel, or both, had lower compressive strengths than Batches B6 to B22–3%HF. Table 4.2 also shows that the baseline mixture, Batch B8–Baseline, had the greatest compressive strength, with a 1-day strength of 13.2 ksi and 28-day strength of 19.6 ksi. Batches B17 to B22–3%HF were only tested for 28-day strength, with the results varying between 13.5 and 16.4 ksi. Clearly, further refinement of the mixture design is warranted to improve its repeatability. As expected, increasing the percentage of fibers, and using hooked fibers, did not have a clear effect on compressive strength.

Table 4.2: Compressive Strengths for All Batches

Batch I.D. / Strength	1 day (ksi)	3 day (ksi)	4 day (ksi)	7 day (ksi)	14 day (ksi)	28 day (ksi)
B1–FlyAsh	10.8	-	-	12.1	13.5	-
B2–FlyAsh	8.8	9.4	-	10.0	11.7[1]	-
B3–PeaGravel	8.7	-	10.5	11.8	12.1	-
B4–FlyAsh	9.0[1]	11.2[1]	-	11.0[1]	12.2[1]	12.1[1]
B5–FlyAsh	9.9	-	10.4	11.4	12.0[1]	12.5[1]
B6	12.7	13.3	-	13.8	14.2	15.0
B7–Fibers2%	12.5	-	15.3	14.7	16.2	16.5
B8–Baseline	13.2	14.8	-	16.8	18.1[1]	19.6
B9–SCA2%	13.0	-	14.3	16.1	16.6	17.8
B10–SCA6%	11.5	13.7	-	15.2	16.0	17.4
B11–SCA10%	12.1	-	14.8	15.5	16.2	17.5
B12–SRA0.5%	12.2	-	-	15.1	15.5	18.1
B13–SRA1.25%	11.6	-	14.1	14.4	15.8	17.5
B14–SRA2%	10.6	12.5	-	13.4	15.6	16.7
B15–LWA15%	11.3	-	13.5	15.7[1]	17.6	17.0
B16–LWA30%	10.3	12.3	-	12.8	15.2[1]	15.2
B17	-	-	-	-	-	15.4
B18–3%SF	-	-	-	-	-	13.5
B19–2%HF	-	-	-	-	-	14.0[1]
B20–2%HF	-	-	-	-	-	15.2[1]
B21–3%HF	-	-	-	-	-	15.0[1]
B22–3%HF	-	-	-	-	-	16.4[1]

[1]Values based on one specimen.

Figures 4.3 to 4.6 show compressive strength versus age at testing for different groups of batches. Batches were grouped as follows: batches with no fibers, batches with SRAs, batches with SCAs, and batches with LWA. Batches within each group were compared to each other and to the baseline mixture, Batch B8–Baseline. The student's t-test was used to quantify whether differences in 28-day strengths were statistically significant. Batches with fewer than two data points for the 28-day strength were not analyzed using the student's t-test.

Figure 4.3 shows the compressive strength of Batch B8–Baseline and the strengths of Batches B1–FlyAsh to B6. Batch B8–Baseline had a statistically higher compressive strength than Batches B4–FlyAsh, B5–FlyAsh, and B6 (p = 0.013). As shown in the figure, Batch 6 had the

highest compressive strength among the batches with no fibers, but the 28-day compressive strength of Batch B6 was still statistically significantly lower than Batch B8–Baseline ($p = 0.042$). Because factors other than fibers differed among these batches, no conclusions can be drawn explaining the differences.

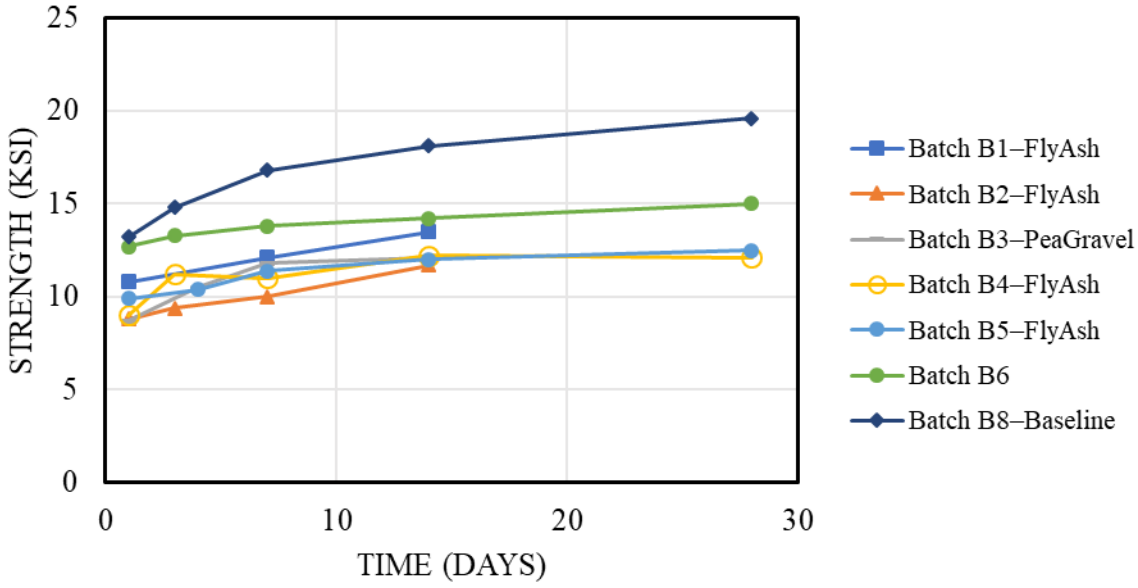

Figure 4.3: Compressive Strength versus Time for Concrete with and without Fibers

Figure 4.4 shows the compressive strength results for Batches B9–SCA2%, B10–SCA6%, and B11–SCA10%, which had different quantities of SCA, and the baseline mixture, Batch B8–Baseline. Batches B9–SCA2%, B10–SCA6%, and B11–SCA10% had, on average, 28-day compressive strengths that were 11% lower than Batch B8–Baseline. This difference was statistically significant ($p < 0.04$). However, no statistically significant difference was found between the 28-day compressive strengths for batches with different dosages of SCA ($p > 0.28$). Other research did not indicate a reduction in compressive strength when adding SCA to conventional concrete (Feng & Darwin, 2020). It is not clear whether the strength reductions observed here are attributable to the SCA or other factors.

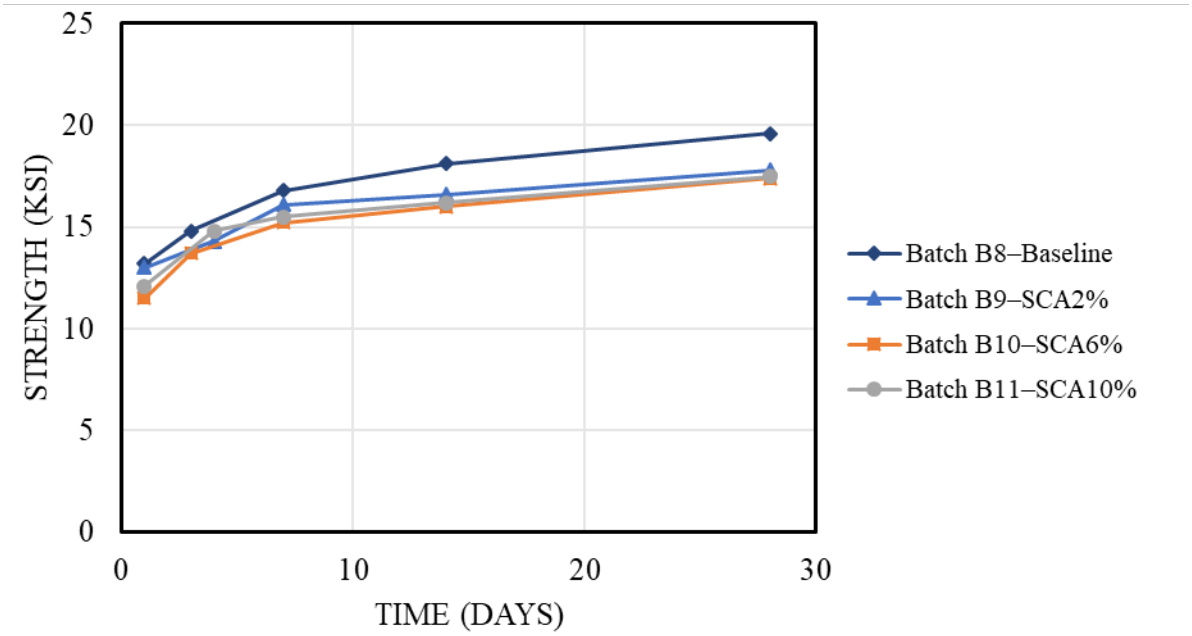

Figure 4.4: Compressive Strength versus Time for Concrete with and without SCAs

Figure 4.5 shows the compressive strengths of Batches B12–SRA0.5%, B13–SRA1.25%, and B14–SRA2%, which had different quantities of SRA, and Batch B8–Baseline. As with the use of SCAs, the use of SRAs was correlated with lower compressive strengths relative to Batch B8–Baseline. The reduction in strength associated with adding any amount of SRA (average of 11%) was statistically significant compared to Batch B8–Baseline ($p < 0.045$). No statistically significant differences were observed between the 28-day compressive strengths of batches with various dosages of SRAs ($p > 0.18$). Previous research has also indicated that the use of SRAs can lead to lower UHPC strength (Liu et al., 2017).

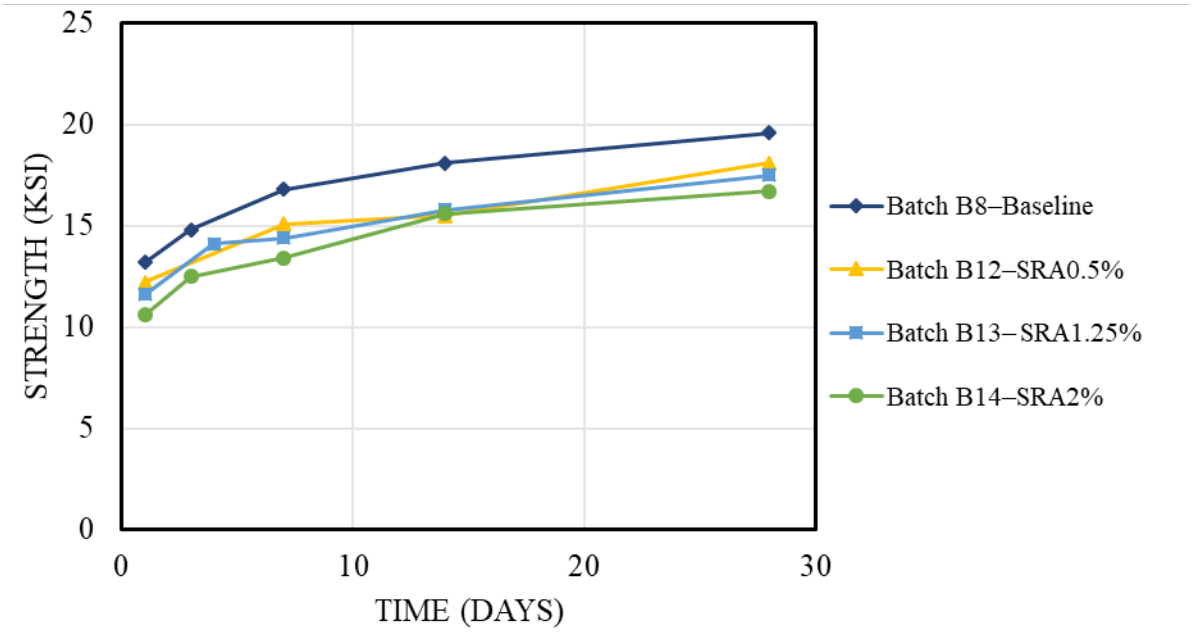

Figure 4.5: Compressive Strength versus Time for Concrete with and without SRAs

Figure 4.6 shows the compressive strength results for batches B15–LWA15% and B16–LWA30%, which had different quantities of LWA, and Batch B8–Baseline. The 1-day strengths for 15% and 30% dosages of LWA were 11.3 ksi and 10.3 ksi, respectively, compared to 13.2 ksi for Batch B8–Baseline, and the 28-day strengths were 17 ksi and 15.2 ksi, respectively, compared to 19.6 ksi for Batch B8–Baseline. The reduction in strength associated with any LWA dosage was statistically significant compared to Batch B8–Baseline ($p < 0.028$), but no statistically significant difference was found between Batches B15–LWA15% and B16–LWA30% ($p = 0.14$). Although previous research has shown an increase in compressive strength associated with adding LWA (Meng & Khayat, 2017), among the three shrinkage-limiting methods in this study, the highest reduction in strength was associated with the use of LWA. It is not clear why LWA had a different effect in this study.

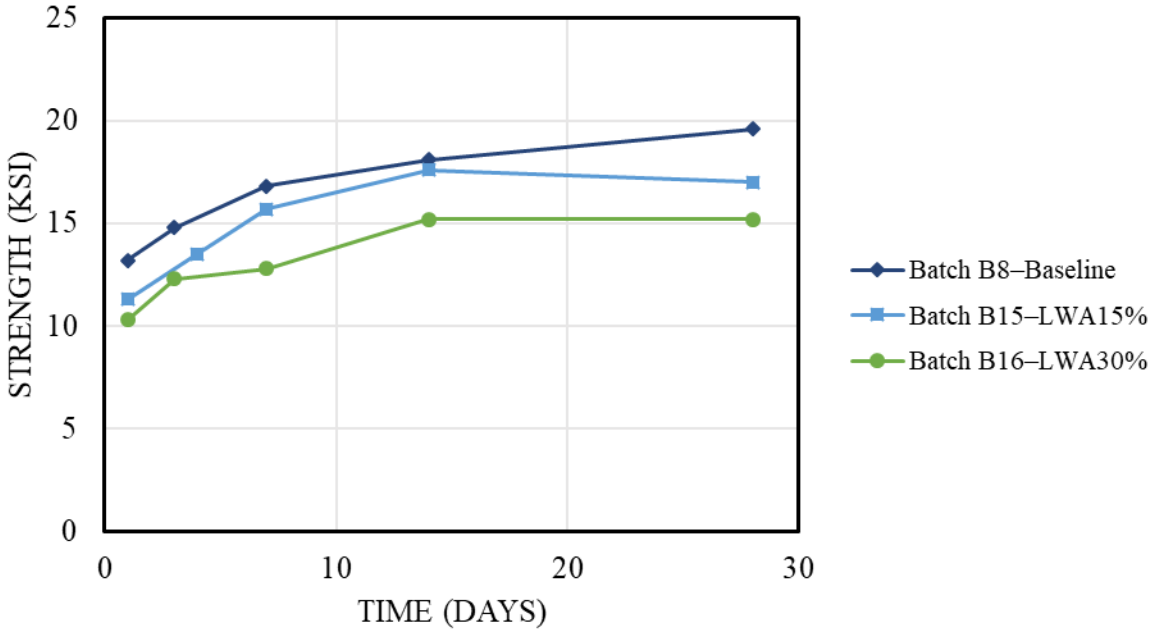

Figure 4.6: Compressive Strength versus Time for Concrete with and without LWA

4.2.2 Compressive Stress-Strain Results

Figure 4.7 shows the stress-strain results up to peak compressive strength of two cylinders from Batch B17 (with 2% by volume of straight fibers) 28 days after mixing. This was the only batch for which strains were measured during a compression test. The post-peak response was not plotted due to data collection issues. The cylinders failed at stresses of 16.8 ksi and 13.2 ksi, at strains of 0.0029 and 0.0019, respectively. The moduli of elasticity of B17-1 and B17-2 were calculated in accordance with ASTM C469-14e (ASTM, 2014). Specimen B17-1 had a modulus of elasticity of 8,300 ksi, and specimen B17-2 had a modulus of elasticity of 6,300 ksi. Equation 4.1, which is based on Equation 19.2.2.1.b (ACI 318-19), would estimate the elastic moduli to be 7,390 ksi for B17-1 and 6,550 ksi for B17-2, which are both within 10% of the experimentally obtained values. Considerably more data are needed to assess the use of Equation 4.1 for estimating the modulus of UHPC, but the equation was relatively accurate in this case.

$$E = 57,000\sqrt{f'_c}\ \text{[psi]}$$

Equation 4.1

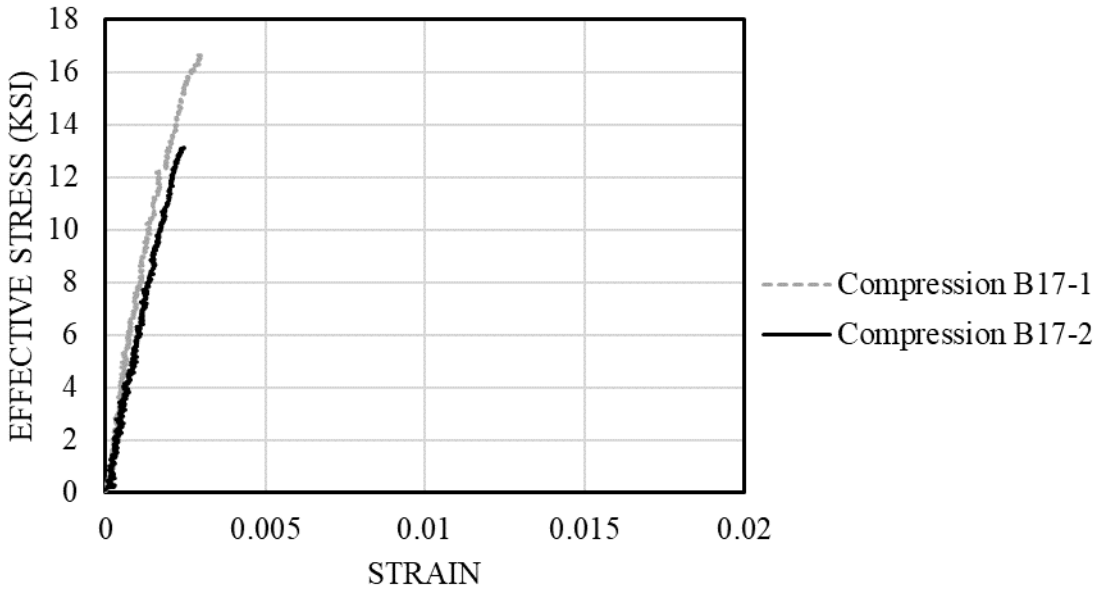

Figure 4.7: Stress versus Strain in Compression for Batch B17

4.2.3 Free Shrinkage

Table 4.3 summarizes the free shrinkage results for Batches B2–PeaGravel to B16–LWA30% at 7, 28, and 90 days. Average shrinkage for the baseline mixture was 687 microstrain at 90 days after mixing, with day one being the reference measurement. Although 687 microstrain is large relative to values commonly obtained for conventional concrete (Feng & Darwin, 2020), it is smaller than values observed in some prior studies of UHPC. For example, Liu et al. (2017) measured shrinkage as high as 900 microstrain at 8 days.

Table 4.3: Free Shrinkage Measurements at 7, 28, and 90 Days

Time (days)	7	28	90
Batch I.D.	**Free Shrinkage (microstrain)**		
B2– PeaGravel	307	467	660
B3– PeaGravel	-	-	-
B4–FlyAsh	120	470	590
B5– FlyAsh	360	490	647
B6	270	517	620
B7– Fibers2%	153	453	627
B8– Baseline	143	580	687

Time (days)	7	28	90
Batch I.D.	**Free Shrinkage (microstrain)**		
B9– SCA2%	217	579[2]	757
B10– SCA6%	173	409[2]	463
B11– SCA10%	10	165[2]	-1580
B12-SRA0.5%	10	415	715
B13– SRA1.25%	177	453	710
B14–SRA2%	113	400	633
B15–LWA15%	191[1]	670	1097
B16–LWA30%	165	620	840

[1] Values based on one specimen.
[2] Based on interpolated values from measurements taken close to the 28th day.

Figures 4.8 to 4.11 show average free shrinkage versus age after mixing for different groups of batches. Batches were grouped as follows: batches with no fibers, batches with SRAs, batches with SCAs, and batches with LWA. Batches within the same group were compared to each other and to the baseline mixture, Batch B8–Baseline. A student's t-test was used to determine whether the differences in shrinkage at 28 and 90 days were statistically significant. Batches with fewer than two data points for shrinkage were not analyzed using the student's t-test.

Figure 4.8 shows the free shrinkage for Batches B2–PeaGravel to B8–Baseline. All the batches before Batch B7–Fibers2% had no fibers, but other factors could have contributed to their behaviors (Table 3.3). As shown in Figure 4.8, Batches B6 and B8–Baseline had the highest shrinkage from days 30 to 70, while no clear differences were apparent among the other batches. Batches B7–Fibers2% and B8–Baseline both had similar mixture designs, but Batch B7–Fibers2% had 23% less shrinkage than Batch B8–Baseline at 28 days, a difference that was statistically significant (p = 0.001). There was, however, no statistically significant difference found when comparing batches with no fibers to batches with fibers at 28 and 90 days (p = 0.44 and 0.65).

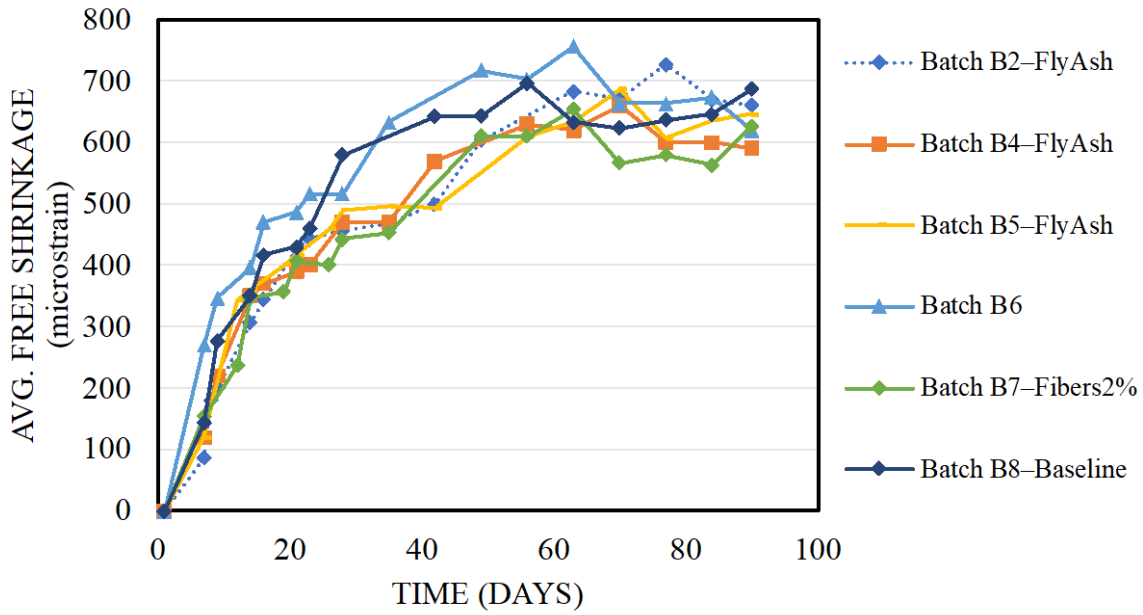

Figure 4.8: Average Free Shrinkage versus Time for Concrete with and without Fibers

Figure 4.9 shows the free shrinkage of Batches B9–SCA2%, B10–SCA6%, and B11–SCA10%, which had different quantities of SCA, and Batch B8–Baseline. Although use of 2% SCA did not effectively limit shrinkage (e.g., Batch B9–SCA2% with 2% SCA exhibited similar shrinkage as Batch B8–Baseline), use of 6% and 10% SCA had a clear effect on reducing shrinkage. Batch B10–SCA6% with 6% SCA exhibited 30% less shrinkage than Batch B8–Baseline at 28 days, and this difference persisted to 90 days after mixing. Batch B11–SCA10% with 10% SCA showed considerable expansion starting from day 35. Although no statistically significant difference in shrinkage was observed between Batches B9–SCA2% and B8–Baseline at 28 or 90 days, the differences between Batch B8–Baseline and Batches B10–SCA6% and B11–SCA10% at 28 days were statistically significant ($p < 4.13\text{E-}04$). The difference between Batches B10–SCA6% and B11–SCA10% were also statistically significant at 28 days ($p < 0.003$).

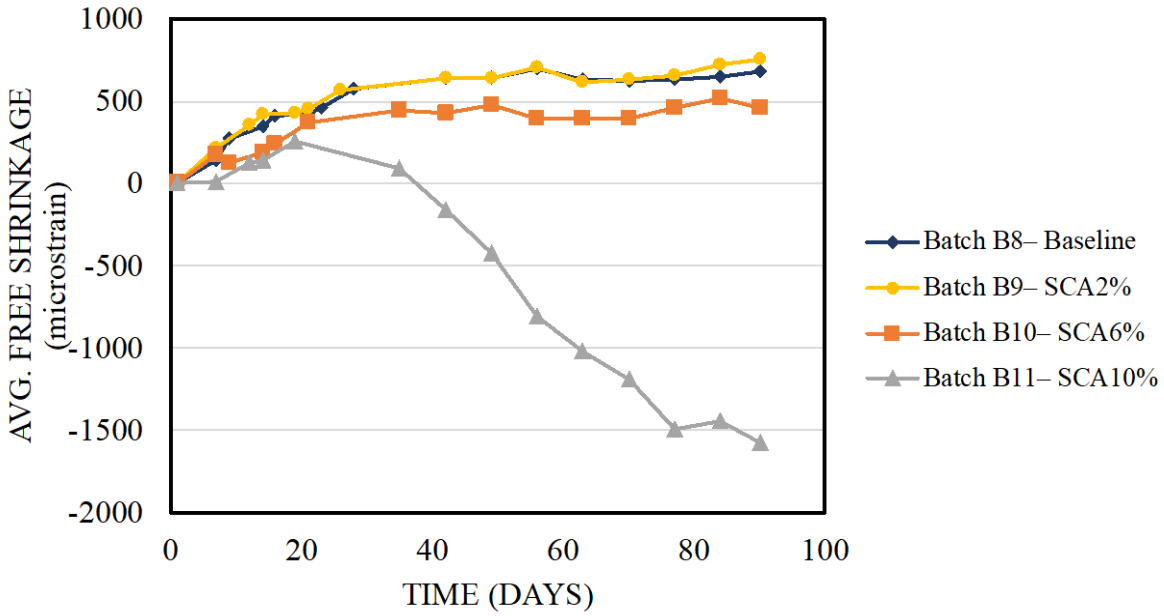

Figure 4.9: Average Free Shrinkage versus Time for Concrete with and without SCA

Figure 4.10 shows the free shrinkage of Batches B12–SRA0.5%, B13–SRA1.25%, and B14–SRA2%, which had different quantities of SRAs, and Batch B8–Baseline. As shown in the figure, the SRA effectively reduced UHPC shrinkage 30 and 60 days after mixing, but no clear differences between Batch B8–Baseline and batches with SRAs were evident 90 days after mixing. Batches B12–SRA0.5%, B13–SRA1.25%, and B14–SRA2% had a statistically significant reduction in shrinkage compared to Batch B8–Baseline at 28 days ($p < 0.003$). However, the difference in shrinkage between Batches B12–SRA0.5%, B13–SRA1.25%, and B14–SRA2% was not statistically significant at 90 days compared to Batch B8–Baseline. All three batches similarly reduced UHPC shrinkage, with no clear effect related to dosage.

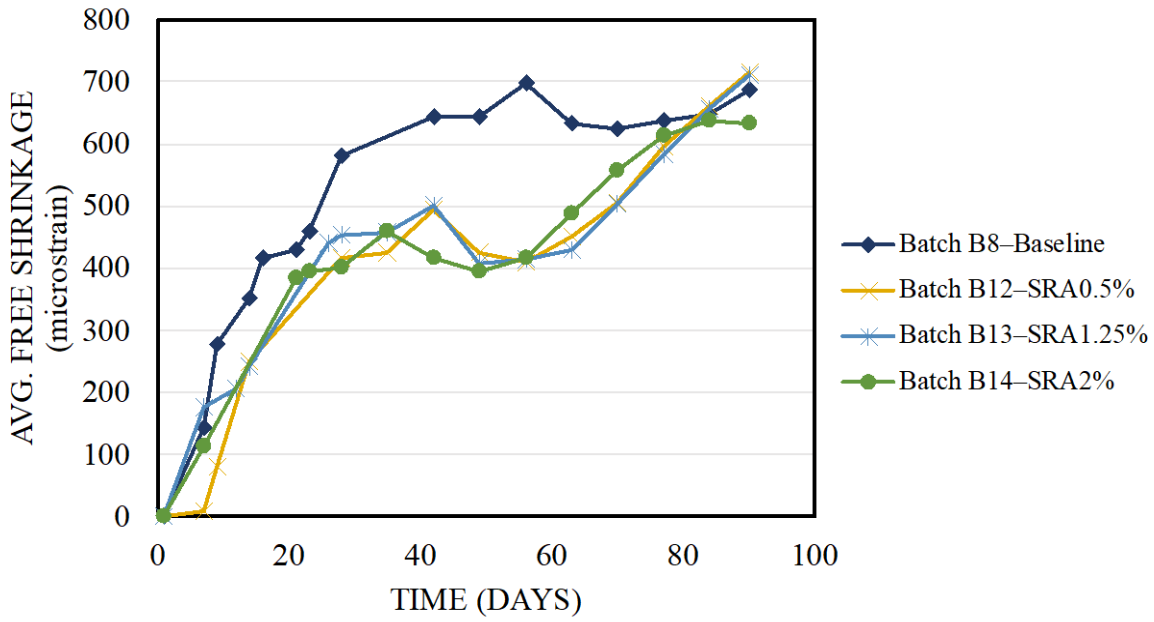

Figure 4.10: Average Free Shrinkage versus Time of Concrete with and without SRA

Figure 4.11 shows the free shrinkage of Batches B15–LWA15% and B16–LWA30%, which had different amounts of LWA, and Batch B8–Baseline. As shown, LWA was not effective in reducing or limiting UHPC shrinkage. Batches B15–LWA15% and B16–LWA30% exhibited more shrinkage at 90 days than Batch B8–Baseline, with Batch B15–LWA15% with 15% LWA exhibiting the greatest shrinkage. The difference in shrinkage between Batches B15–LWA15% and B8–Baseline was statistically significant at 28 and 90 days ($p < 0.005$). LWA was not expected to increase shrinkage, so it was unexpected that the smaller dosage of LWA would have the larger effect on shrinkage. Further study is recommended.

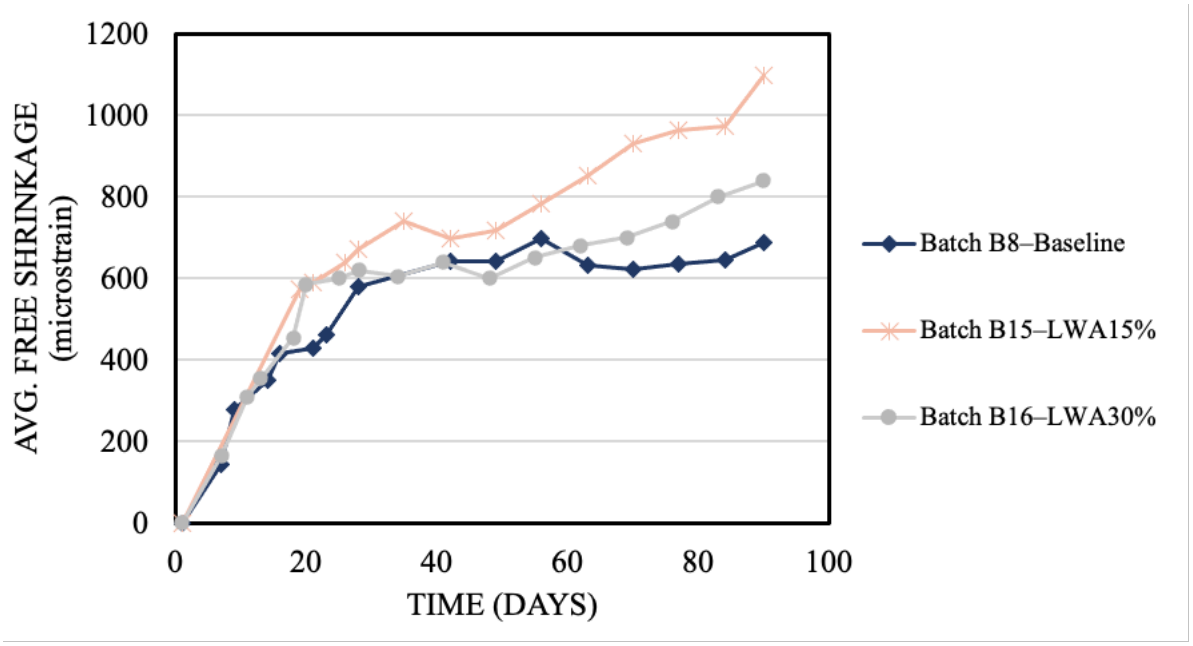

Figure 4.11: Average Free Shrinkage versus Time for Concrete with and without LWA

4.2.4 Direct Tension Tests

Figures 4.12 to 4.14 show the tensile stress versus crack width for specimens from Batches B17, B19–2%HF, B20–2%HF, and B21–3%HF. Results from Batches B18–3%SF and B22–3%HF were not plotted due to data collection issues. Stress was calculated by dividing the force by the cross-sectional area at the notch at the mid-length (based on measured dimensions for each specimen and subtracting the bar area). The reported crack width is the width at the centroid of the specimen estimated based on surface measurements assuming that plane sections stay plane throughout the tests.

These figures show similar trends. For example, crack width remained zero until cracking at approximately 800 to 900 psi in all but one specimen (B20–2%HF-1), which cracked at approximately 600 psi. The specimens all exhibited greater strength after cracking, a behavior known as strain-hardening, which is associated with development of multiple fine cracks in members without notches. The specimens reached their peak stress at 0.018 in. on average for specimens with straight fibers and 0.035 in. on average for specimens with hooked fibers. The larger deflection at peak strength for specimens with hooked fibers was expected because longer fibers are more effective at resisting crack opening than short fibers when crack widths are large.

After peak, all the specimens gradually lost strength, although all still resisted more than 600 psi at crack widths of 0.1 in. except for specimens from Batch B17 and B20–2%HF-1.

Figures 4.12 to 4.14 also show considerable scatter among the specimens within each batch. For example, B17-1 had a peak stress that was 47% higher than B17-2 (Figure 4.12); B20–2%HF-2 had a peak stress that was 24% higher than B20–2%HF-1 (Figure 4.13); and B21–3%HF-1 had a peak stress that was 20% higher than B21–3%HF-2. It is possible this scatter is a result of nonuniform fiber distributions. Batches B17, B20–2%HF, B21–3%HF, and B22–3%HF all exhibited segregation and blocking values greater than 2 in., which would contribute to nonuniform fiber distributions.

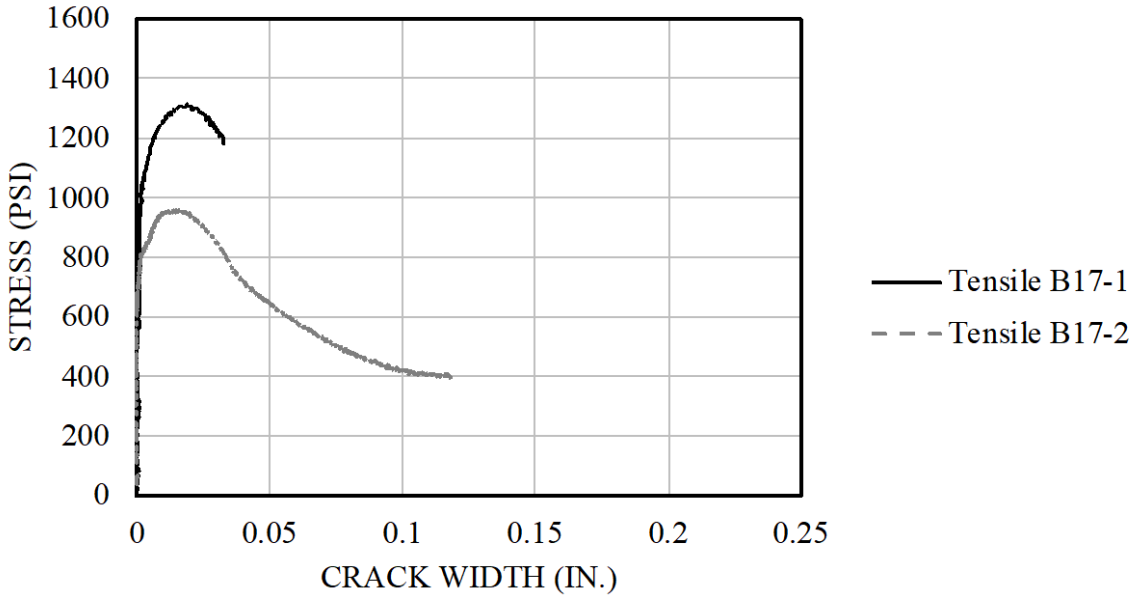

Figure 4.12: Stress versus Crack Width for Batch B17 (2% straight fibers)

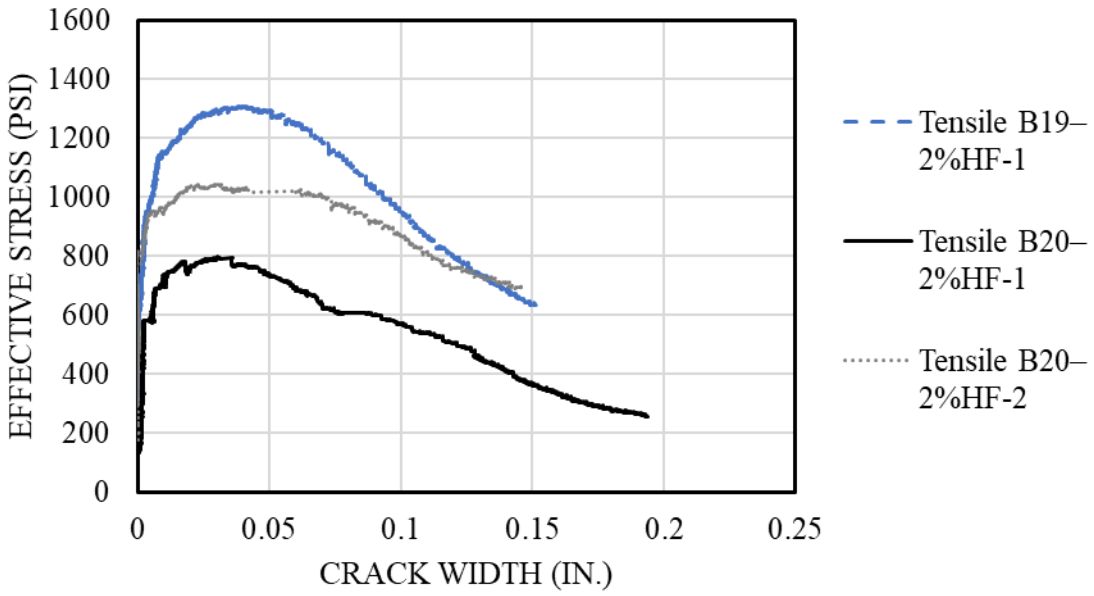

Figure 4.13: Stress versus Crack Width for Batches B19–2%HF and B20–2%HF

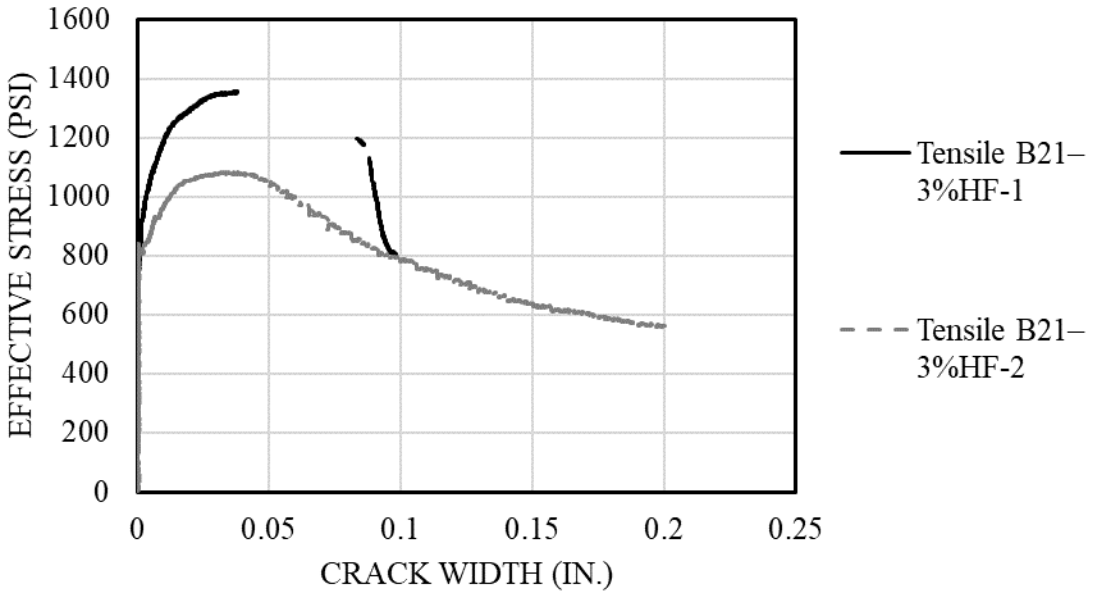

Figure 4.14: Stress versus Crack Width for Batch B21–3%HF

Table 4.4 summarizes the measured stresses for Batches B17, B20–2%HF, B21–3%HF, and B22–3%HF at peak stress and at crack widths of 0.05 and 0.10 in. Considerable scatter is evident: consider the peak stresses measured for specimens B20–2%HF-1, B21–3%HF-1, and B21–3%HF-2, which had the same type and quantity of fiber: 1300, 800, and 1040 psi. This wide

variability is potentially a result of segregation that was observed in Batches B17 to B21–3%HF, which may have resulted in different quantities of fibers at the notched section.

Table 4.5 shows the mean values for specimens with the same fiber type and volume fraction. On average, the specimens with 2% straight and 2% hooked fibers had similar peak stresses. This observation is supported by a student's t-test, which showed no statistically significant difference between these values (p = 0.73). As expected, the batch with 3% hooked fibers had somewhat higher stresses at peak and at crack width of 0.05 in. than the batch with 2% hooked fibers, but these differences were not statistically significant (p = 0.51). Mixtures with hooked fibers tended to have higher stresses at crack widths of 0.05 and 0.10 in. than mixtures with straight fibers, which is expected since the hooked fibers were more than twice as long as the straight fibers (1.2 in. versus 0.5 in.). However, the statistical significance of this difference could not be tested due to insufficient data. The limited test data indicate that straight and hooked fibers might provide similar performance at 2% volume fractions, and that marginal improvements might be realized by increasing the volume fraction to 3%. More research is needed to obtain statistically significant results.

Table 4.4: Summary of Measured Tensile Stresses

Specimen[1]	B17-1	B17-2	B19–2%HF	B20–2%HF-1	B20–2%HF-2	B21–3%HF-1	B21–3%HF-2
Peak Stress (psi)	1310	960	1300	800	1040	1360	1080
Stress at 0.05 in. Crack Width (psi)	-	650	1290	730	1020	1310[2]	1050
Stress at 0.10 in. Crack Width (psi)	-	420	950	570	870	800	780

[1] Batch 17 had 2% straight fibers, Batches 19 and 20 had 2% hooked fibers, Batch 21 had 3% hooked fibers (all percentages are by volume, refer to Table 3.3).
[2] Data missing at 0.05 in., so the value is based on linear interpolation between available values.

Table 4.5: Mean Values of Direct Tension Test Results

Fiber Volume and Type	Mean 2% Straight	Mean 2% Hooked	Mean 3% Hooked
Peak Stress (psi)	1140	1150	1220
Stress at 0.05 in. Crack Width (psi)	650[1]	1010	1180
Stress at 0.10 in. Crack Width (psi)	420[1]	800	790

[1] Based on one value.

Figures 4.15 and 4.16 show specimens B17-1 and B17-2, respectively, after failure. No clear difference was observed between the specimens that would explain the large difference in tensile strength. Nevertheless, fiber distribution within the specimens and across the notched section within a specimen are believed to have contributed to the scatter in the tensile test results.

Figure 4.15: B17 Tensile Specimen 1

Figure 4.16: B17 Tensile Specimen 2

4.2.5 Beam Tests

Figures 4.17 to 4.20 show the effective bending stress versus deflection for beams from Batches B17 to B22–3%HF. Effective bending stress is the stress at the extreme tension fiber calculated from the applied force, assuming an uncracked moment of inertia. Deflection is the difference between the vertical displacement at midspan and the average vertical displacement at the supports. As shown in the figures, specimens with the same fiber type and volume exhibited similar initial slopes, and almost all specimens deviated from linearity (cracked) at extreme tension fiber stresses between 1500 and 2000 psi. Every specimen showed deflection-hardening behavior, meaning that the peak strength exceeded the cracking strength. However, as with the tension test

results, considerable scatter was evident among results from specimens from the same batches, especially as evident in Figure 4.20.

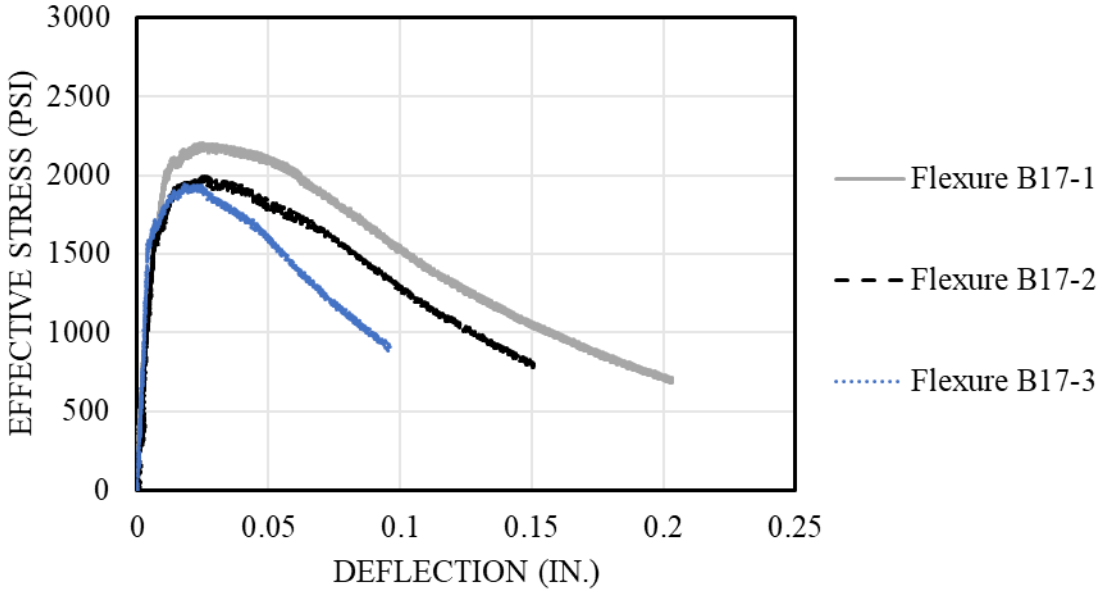

Figure 4.17: Effective Stress versus Deflection for Batch B17 (2% straight fibers)

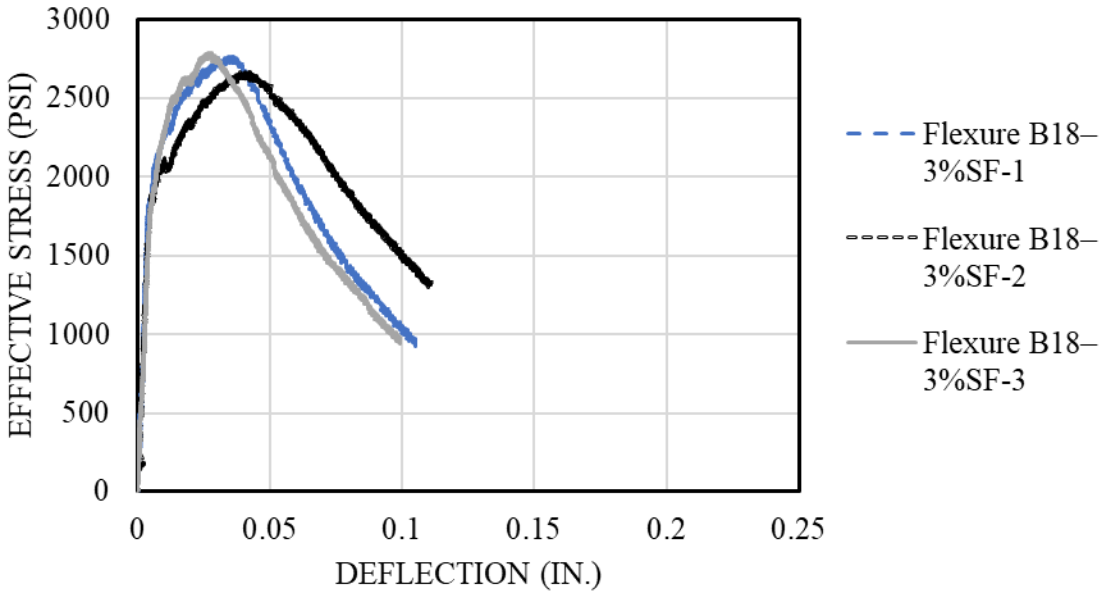

Figure 4.18: Effective Stress versus Deflection for Batch B18–3%SF

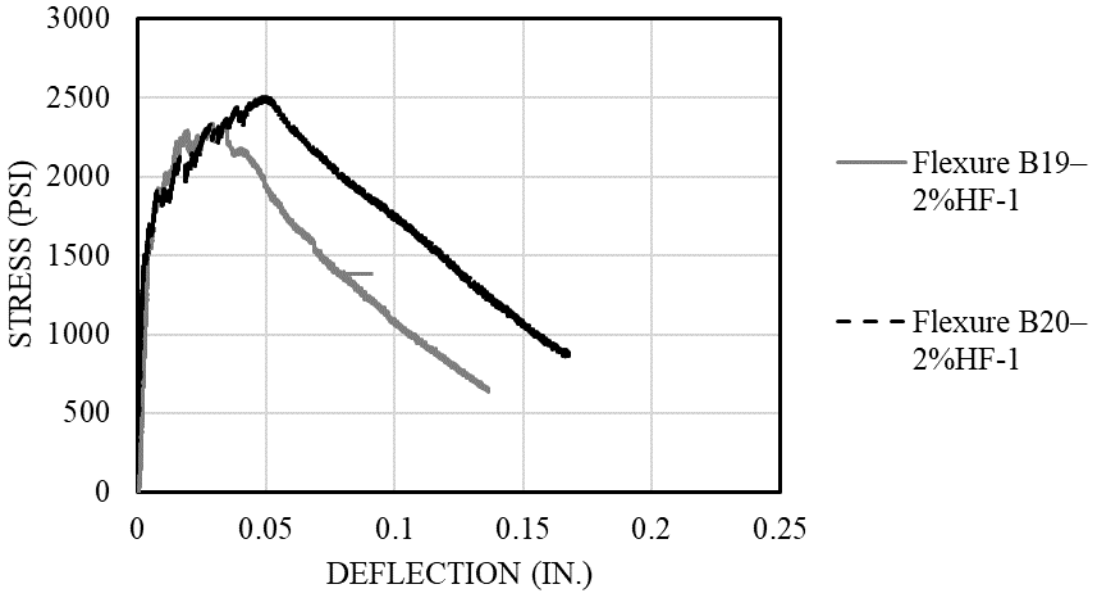

Figure 4.19: Effective Stress versus Deflection for Batches B19–2%HF and B20–2%HF

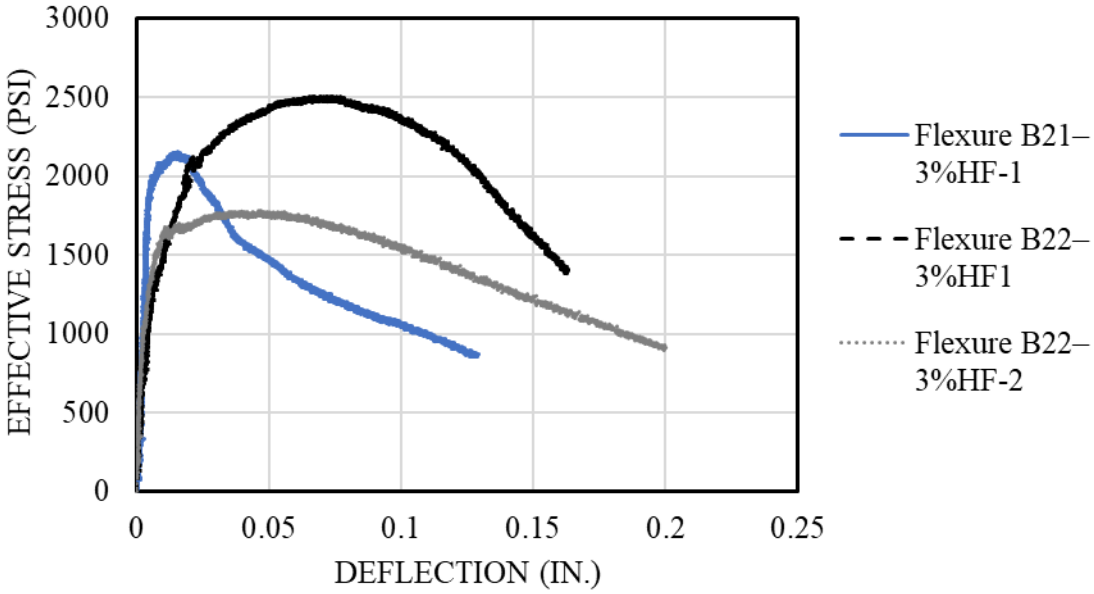

Figure 4.20: Effective Stress versus Deflection for Batches B21–3%HF and B22–3%HF

Table 4.6 summarizes the bending test results in terms of peak effective bending stress, deflection at peak stress, effective bending stresses at 0.04 in. and 0.10 in. deflection, and the ratio of stress at 0.10 in. of deflection to peak stress. Table 4.7 shows the mean values of these parameters for groups of specimens with the same fiber volume and type.

Table 4.6: Summary of Beam Test Results

Specimen[1]	Peak Stress (psi)	Deflection at Peak Stress (in.)	Stress at 0.04 in. Deflection (psi)	Stress at 0.10 Deflection (psi)	Ratio of Stress at 0.10 in. to Peak Stress
B17-1	2200	0.025	2150	1530	0.70
B17-2	1990	0.025	1920	1290	0.65
B17-3	1940	0.018	1750	860	0.44
B18–3%SF-1	2750	0.035	2680	1050	0.38
B18–3%SF-2	2660	0.042	2650	1520	0.57
B18–3%SF-3	2780	0.028	2480	940	0.34
B19–2%HF-1	2300	0.029	2170	1060	0.46
B20–2%HF-1	2500	0.05	2370	1750	0.70
B21–3%HF-1	2150	0.016	1580	1060	0.49
B22–3%HF-1	2500	0.07	2350	2360	0.94
B22–3%HF-2	1770	0.048	1770	1550	0.87

[1] Batch 17 had 2% straight fibers, Batch 18 had 3% straight fibers, Batches 19 and 20 had 2% hooked fibers, Batches 21 and 22 had 3% hooked fibers (all percentages are by volume, refer to Table 3.3).

Table 4.7: Mean Values of Beam Test Results

Fiber Volume and Type	Peak Stress (psi)	Deflection at Peak Stress (in.)	Stress at 0.04 in. Deflection (psi)	Stress at 0.10 Deflection (psi)
Mean 2% Straight	2040	0.023	1940	1230
Mean 3% Straight	2730	0.035	2600	1170
Mean 2% Hooked	2400	0.04	2270	1410
Mean 3% Hooked	2140	0.045	1900	1660

Tables 4.6 and 4.7 do not indicate clear trends. While increasing the volume fraction of straight fibers from 2% to 3% had a statistically significant correlation with increased stresses at peak and at 0.04 in. deflection ($p \leq 0.007$), the opposite appeared true when comparing specimens with 2% and 3% volume fractions of hooked fibers. Given the high scatter and inconsistent results, additional data are necessary to conclude whether straight and hooked fibers are interchangeable. No statistically significant difference was found when batches with hooked fibers were compared to batches with straight fibers ($p > 0.20$).

Chapter 5: Summary and Conclusions

Results are reported from tests on 22 batches of nonproprietary ultra-high-performance concrete (UHPC). The aims of this work were to (1) develop a nonproprietary UHPC mixture design using primarily Kansas-based materials that rapidly gains strength for use in accelerated bridge construction and (2) explore the effectiveness of using shrinkage reducing admixtures (SRAs), shrinkage compensating admixtures (SCAs), and lightweight aggregate (LWA) to reduce UHPC shrinkage. Low-shrinkage UHPC is desirable because it has the potential to limit crack widths between UHPC pour-strips and adjoining precast beams. Limited tests are also reported that quantify the tensile and flexural response of UHPC with different quantities of high-strength straight and hooked steel fibers. The findings justify the following conclusions:

1. UHPC can be produced with conventional mixing equipment using primarily Kansas-based materials and the mixture design outlined in Table 3.1. These mixture proportions produced concrete with 1-, 7-, and 28-day compressive strengths as high as 13.1, 16.8, and 19.6 ksi, respectively. There was, however, some difficulty reproducing these results, suggesting that further mixture design refinement is needed to improve its robustness/repeatability. The mixture proportions provided good workability, with slump flow values consistently greater than 23 in. based on testing done in accordance with ASTM C1611 (ASTM, 2021).
2. The SRA used in this study effectively reduced UHPC shrinkage by approximately one-third between 30 and 60 days but had no statistically significant effect on shrinkage measured 90 days after mixing. No clear correlation was observed between shrinkage and SRA dosage for the quantities used in this study. SRAs may not be the best option for controlling shrinkage of UHPC in pour-strip applications, where crack width at the joint between the UHPC and precast beam is the primary

concern. In these applications, long-term shrinkage control is more important than temporary early-age shrinkage control.

3. The SCA used in this study effectively reduced UHPC shrinkage when sufficiently high dosages were used. Although a 2% dosage had no observed effect on shrinkage, a 6% dosage reduced UHPC shrinkage by approximately one-third between 28 and 90 days after mixing. The batch with 10% SCA exhibited considerable expansion between 35 and 90 days after mixing. SCAs are able to reduce shrinkage of UHPC throughout the time periods considered in this study and are therefore recommended for use in pour strips when shrinkage is a concern.
4. The use of prewetted LWA did not effectively reduce shrinkage in this study, and its usage was correlated with reduced compressive strength in limited tests. These results contribute to the inconsistent results reported in prior research. Further research is needed.
5. The UHPC in this study exhibited its peak tensile strength after cracking (referred to as tension hardening behavior). The limited test data indicate that straight and hooked fibers might provide similar tensile strengths at 2% volume fractions, and that marginal improvements can be realized by increasing the volume fraction to 3%. The limited data also show that 1.2-in.-long hooked fibers exhibited greater strength than 0.5-in.-long straight fibers at crack widths of 0.05 and 0.10 in. Further study is needed to obtain statistically significant results.
6. All beam tests exhibited deflection hardening consistent with multiple cracking. Due to the considerable scatter that was observed, no further conclusions were made on the basis of the bending test results.

References

ACI Committee 209. (2005). *Report on factors affecting shrinkage and creep of hardened concrete* (ACI 209.1R-05). American Concrete Institute.

Aghdasi, P., Heid, A. E., & Chao, S.-H. (2016). Developing ultra-high performance fiber-reinforced concrete for large-scale structural applications. *ACI Materials Journal*, *113*(5), 559-570. https://doi.org/10.14359/51689103

Alkaysi, M., & El-Tawil, S. (2016). Effects of variations in the mix constituents of ultra-high performance concrete (UHPC) on cost and performance. *Materials and Structures*, *49*, 4185-4200. https://doi.org/10.1617/s11527-015-0780-6

Alsalman, A., Dang, C. N., Martí-Vargas, J. R., & Hale, W. M. (2020). Mixture-proportioning of economical UHPC mixtures. *Journal of Building Engineering*, *27*. https://doi.org/10.1016/j.jobe.2019.100970

ASTM A820/A820M-16. (2016). *Standard specification for steel fibers for fiber-reinforced concrete*. ASTM International. 10.1520/A0820_A820M-16, https://www.astm.org

ASTM C33/C33M-18. (2018). *Standard specification for concrete aggregates*. ASTM International. 10.1520/C0033_C0033M-18, https://www.astm.org

ASTM C39/C39M-21. (2021). *Standard test method for compressive strength of cylindrical concrete specimens.* ASTM International. 10.1520/C0039_C0039M-21, https://www.astm.org

ASTM C138/C138M-17a. (2017). *Standard test method for density (unit weight), yield, and air content (gravimetric) of concrete.* ASTM International. 10.1520/C0138_C0138M-17a, https://www.astm.org

ASTM C150/C150M-21. (2021). *Standard specification for portland cement.* ASTM International. 10.1520/C0150_C0150M-21, https://www.astm.org

ASTM C157/C157M-17. (2017). *Standard test method for length change of hardened hydraulic-cement mortar and concrete.* ASTM International. 10.1520/C0157_C0157M-17, https://www.astm.org

ASTM C469/C469M-14e. (2021). *Standard test method for static modulus of elasticity and poisson's ratio of concrete in compression.* ASTM International. 10.1520/C0469_C0469M-14E01, https://www.astm.org

ASTM C494/C494M-19. (2019). *Standard specification for chemical admixtures for concrete*. ASTM International. 10.1520/C0494_C0494M-19, https://www.astm.org

ASTM C618-19. (2019). *Standard specification for coal fly ash and raw or calcined natural pozzolan for use in concrete*. ASTM International. 10.1520/C0618-19, https://www.astm.org

ASTM C1064/C1064M-17. (2017). *Standard test method for temperature of freshly mixed hydraulic cement concrete.* ASTM International. 10.1520/C1064_C1064M-17, https://www.astm.org

ASTM C1240-20. (2020). *Standard specification for silica fume used in cementitious mixtures.* ASTM International. 10.1520/C1240-20, https://www.astm.org

ASTM C1609/C1609M-19a. (2019). *Standard test method for flexural performance of fiber-reinforced concrete (using beam with third-point loading).* ASTM International. 10.1520/C1609_C1609M-19a, https://www.astm.org

ASTM C1611/C1611M-21. (2021). *Standard test method for slump flow of self-consolidating concrete.* ASTM International. 10.1520/C1611_C1611M-21, https://www.astm.org

ASTM C1621/C1621M-17. (2017). *Standard test method for passing ability of self-consolidating concrete by j-ring.* ASTM International. 10.1520/C1621_C1621M-17, https://www.astm.org

ASTM C1856/C1856M-17. (2017). *Standard practice for fabricating and testing specimens of ultra-high performance concrete.* ASTM International. 10.1520/C1856_C1856M-17, https://www.astm.org

Castine, S. (2017). *Development of high early-strength concrete for accelerated bridge construction closure pour connections* (Report No. 498) (Master's thesis). University of Massachusetts Amherst. https://doi.org/10.7275/9882696

Chen, W., & Brouwers, H. J. H. (2012). Hydration of mineral shrinkage-compensating admixture for concrete: An experimental and numerical study. *Construction and Building Materials, 26*, 670-676. https://doi.org/10.1016/j.conbuildmat.2011.06.070

Čítek, D., Rydval, M., & Kolísko, J. (2016). Volumetric changes of the UHPC matrix and its determination. *Applied Mechanics and Materials*, *827*, 215-218. http://dx.doi.org/10.4028/www.scientific.net/AMM.827.215

Deboodt, T., Fu, T., & Ideker, J. (2016). Evaluation of FLWA and SRAs on autogenous deformation and long-term drying shrinkage of high performance concrete. *Construction and Building Materials*, *119*, 53-60. https://doi.org/10.1016/j.conbuildmat.2016.05.068

Feng, M., & Darwin, D. (2020). *Implementation of crack-reducing technologies for concrete in bridge decks: Synthetic fibers, internal curing, and shrinkage-reducing admixtures* (SM Report No. 136). University of Kansas Center for Research. hdl.handle.net/1808/30243

Floyd, R. W., Volz, J. S., Zaman, M., Dyachkova, Y., Roswurm, S., Choate, J., Looney, T., & Walker, C. (2020). *Development of non-proprietary UHPC mix: Quarterly progress report for the period ending February 29, 2020*. Submitted to the Accelerated Bridge Construction University Transportation Center (ABC-UTC) at Florida International University. https://abc-utc.fiu.edu/wp-content/uploads/2020/04/OU-2016-2-1_Non-Proprietary-UHPC-ProgressReportQ4_03_31_2020.pdf

Graybeal, B. (2008). UHPC in the U.S. highway transportation system. In E. Fehling, M. Schmidt, & S. Stürwald (Eds.), *Ultra high performance concrete (UHPC): Proceedings of the Second International Symposium on Ultra High Performance Concrete, Kassel, Germany, March 05-07, 2008*, (11-17). Kassel University Press. https://www.uni-kassel.de/upress/online/frei/978-3-89958-376-2.volltext.frei.pdf

Justs, J., Wyrzykowski, M., Bajare, D., & Lura, P. (2015). Internal curing by superabsorbent polymers in ultra-high performance concrete. *Cement and Concrete Research*, *76*, 82-90. https://doi.org/10.1016/j.cemconres.2015.05.005

Lafikes, J., Darwin, D., & O'Reilly, M. (2020). *Durability, construction, and early evaluation of low-cracking high-performance concrete (LC-HPC) bridge decks* (SM Report No. 141). University of Kansas Center for Research. hdl.handle.net/1808/30571

Li, M., Liu, J., Tian, Q., Wang, Y., & Xu, W. (2017). Efficacy of internal curing combined with expansive agent in mitigating shrinkage deformation of concrete under variable temperature condition. *Construction and Building Materials*, *145*, 354-360. https://doi.org/10.1016/j.conbuildmat.2017.04.021

Liu, J., Shi, C., Ma, X., Khayat, K., Zhang, J., & Wang, D. (2017). An overview on the effect of internal curing on shrinkage of high-performance cement-based materials. *Construction and Building Materials, 146*, 702-712. http://dx.doi.org/10.1016/j.conbuildmat.2017.04.154

Magureanu, C., Sosa, I., Negrutiu, C., & Heghes, B. (2012). Mechanical properties and durability of ultra-high-performance concrete. *ACI Materials Journal*, *109*(2), 177-184. https://doi.org/10.14359/51683704

Meng, W., & Khayat, K. (2017). Effects of saturated lightweight sand content on key characteristics of ultra-high-performance concrete. *Cement and Concrete Research*, *101*, 46-54. https://doi.org/10.1016/j.cemconres.2017.08.018

Meng, W., Valipour, M., & Khayat, K. H. (2016). Optimization and performance of cost-effective ultra-high performance concrete. *Materials and Structures*, *50*. http://dx.doi.org/10.1617/s11527-016-0896-3

Mindess, S., Young, J. F., & Darwin, D. (2003). *Concrete* (2nd ed.). Pearson Education Inc.

Pendergrass, B., & Darwin, D. (2014). *Low-cracking high-performance concrete (LC-HPC) bridge decks: Shrinkage-reducing admixtures, internal curing, and cracking performance* (SM Report No. 107). University of Kansas Center for Research. hdl.handle.net/1808/19821

Pendergrass, B., Darwin, D., Khajehdehi, R., & Feng, M. (2017). *Combined effects of internal curing, slag, and silica fume on drying shrinkage of concrete* (SL Report No. 17-1). University of Kansas Center for Research. hdl.handle.net/1808/25916

Tameemi, W. & Lequesne, R. (2015). *Correlations between compressive, flexural, and tensile behavior of self-consolidating fiber reinforced concrete* (SM Report No. 114). University of Kansas Center for Research. hdl.handle.net/1808/19741

Tameemi, W., Perez-Irizarry, A. L., Dudnik, V., Lequesne, R. D., & Parra-Montesinos, G. J. (2016, September 19 – 21). *Correlations between results from compressive, flexural, and tensile tests of steel fiber reinforced concrete* [Conference presentation]. BEFIB2016 – 9th RILEM International Symposium on Fiber Reinforced Concrete, Vancouver, British Columbia, Canada.

Teng, L., Valipour, M., & Khayat, K. H. (2021). Design and performance of low shrinkage UHPC for thin bonded bridge deck overlay. *Cement and Concrete Composites*, *118*. https://doi.org/10.1016/j.cemconcomp.2021.103953

Wille, K., & Boisvert-Cotulio, C. (2015). Material efficiency in the design of ultra-high performance concrete. *Construction and Building Materials*, *86*, 33-43. https://doi.org/10.1016/j.conbuildmat.2015.03.087

Wille, K., Naaman, A. E., & El-Tawil, S. (2011a). Optimizing ultra-high-performance fiber-reinforced concrete. *Concrete International*, *33*(9), 35-41. https://www.researchgate.net/publication/284685717_Optimizing_ultra-high-performance_fiber-reinforced_concrete

Wille, K., Naaman, A. E., & Parra-Montesinos, G. J. (2011b). Ultra-high performance concrete with compressive strength exceeding 150 MPa (22 ksi): A simpler way. *ACI Materials Journal*, *108*(1), 46-54. https://doi.org/10.14359/51664215

Xie, T., Fang, C., Mohamad Ali, M. S., & Visintin, P. (2018). Characterizations of autogenous and drying shrinkage of ultra-high performance concrete (UHPC): An experimental study. *Cement and Concrete Composites*, *91*, 156-173. https://doi.org/10.1016/j.cemconcomp.2018.05.009

Yuan, J., & Graybeal, B. (2014). *Bond behavior of reinforcing steel in ultra-high performance concrete* (Report No. FHWA-HRT-14-090). Federal Highway Administration. https://www.fhwa.dot.gov/publications/research/infrastructure/structures/bridge/14090/index.cfm

Yuan, J., & Graybeal, B. (2015). Bond of reinforcement in ultra-high-performance concrete. *ACI Structural Journal, 112*(6), 851-860. https://doi.org/10.14359/51687912

Appendix A

Materials	Batch I.D.						
	B1– FlyAsh	B2 – PeaGravel	B3– PeaGravel	B4– FlyAsh	B5– FlyAsh	B6	B7– Fibers2 %
Cement	1189	1158	1158	1146	1154	1410	1387
Silica Fume	297	290	290	286	288	283	279
Fly Ash	289	281	281	278	-	-	-
Pea Gravel	0	521	521	-	-	-	-
Fine Agg.	1784	1218	1220	1797	1811	1977	1944
Water	376	373	371	328	330	324	319
HRWR	23	21	21	21	24	24	25
HRWR dosage	18.9	17.8	18.2	18.2	24.6	20.7	22.1
Fibers	-	-	-	-	-	-	269
SCA	-	-	-	-	-	-	-
SRA	-	-	-	-	-	-	-
LWA	-	-	-	-	-	-	-

Materials	Batch I.D.					
	B8 – Baseline	B9– SCA2%	B10– SCA6%	B11– SCA10%	B12– SRA0.5%	B13– SRA1.25 %
Cement	1362	1356	1376	1388	1393	1369
Silica Fume	274	272	276	279	282	275
Fly Ash	-	-	-	-	-	-
Pea Gravel	-	-	-	-	-	-
Fine Agg.	1909	1906	1849	1832	1994	1919
Water	312	311	314	314	319	284
HRWR	26	26	28	34	28	28

HRWR dosage	23.3	23.4	24.8	30.1	24.9	24.8
Fibers 1	265	263	267	269	273	266
SCA	-	34	102	172	-	-
SRA	-	-	-	-	8	28
LWA	-	-	-	-	-	-

Materials	**Batch I.D.**				
	B14–SRA2%	B15–LWA15%	B16–LWA30%	B17	B18–3%SF
Cement	1358	1424	1351	1355	1297
Silica Fume	273	286	271	272	261
Fly Ash	-	-	-	-	-
Pea Gravel	-	-	-	-	-

Materials	**Batch I.D.**				
	B19–2%HF	B20–2%HF	B21–2%HF	B22–3%HF	KDOT-Testing
Cement	1365	1371	1352	1366	1362
Silica Fume	274	275	272	274	274
Fly Ash	-	-	-	-	-
Pea Gravel	-	-	-	-	-
Fine Agg.	1909	1918	1894	1914	1917
Water	299	300	287	290	304
HRWR	65	63	63	55	27
HRWR dosage	58.2	56.2	57.2	49.3	24.1
Fibers 1	-	-	-	-	264
Hooked Fibers	265	266	398	402	-
SCA	-	-	-	-	-
SRA	-	-	-	-	-
LWA	-	-	-	-	-

Fine Agg.	1904	1517	987	1900	1818
Water	276	302	283	309	286
HRWR	29	30	27	54	82
HRWR dosage	26.1	25.8	24.1	48.4	77.1
Fibers 1	264	276	262	-	-
Fibers 2	-	-	-	263	382
SCA	-	-	-	-	-
SRA	33	-	-	-	-
LWA	-	254	486	-	-

Appendix B

REPORT OF RESULTS:

KU UHPC

UHPC Mixture Design for Accelerated Bridge Construction

Bureau of Research

Wadley, Mayer, McArtor

May 2021 – September 2021

Kansas Department of Transportation

Materials and Research Center

2300 SW Van Buren St.

Topeka, KS 66611-1195

TABLE OF CONTENTS

1. OVERVIEW OF KDOT TESTING

KDOT conducted testing on two UHPC mixtures designed by the University of Kansas Research Team: 1) UHPC mix at KU on May 19, 2021, and 2) UHPC mix at KDOT MRC on September 29, 2021. An overview of the tests conducted for each UHPC mix are described in the following sections.

1.1 UHPC Mix at KU – 5/19/2021 (MRC# 21-0902)

This mix was done at KU on May 19, 2021, by the KU Research Team. The KDOT Research team attended the mix to watch and collect samples to conduct hardened property testing. Specimens were prepared by the KU research team and transported to KDOT for testing. The following table summarizes the samples tested by KDOT.

Table 1-1: UHPC Samples Tested by KDOT

Test	Day of Test	Sample Size	No. of Samples Made
Volume of Permeable Voids (KT-73)	28 d	4”x8” cylinder	2
Rapid Chloride Permeability (AASHTO T 277)	56 d	4”x8” cylinder	2
Surface Resistivity (KT-79)	28 d	4”x8” cylinder	Used V.P.V. cylinders
Hardened Air (ASTM C 457)	28 d	4”x8” cylinder	2
Freeze-Thaw (KTMR-22)	Varies	3”x4”x16” beam	3 cut, 3 uncut
Temperature (iButton)	--	4”x8” cylinder	2
		Total No. of Samples =	**8 cyls, 6 beams**

1.2 UHPC Mix at KDOT MRC – 9/29/2021 (MRC# 21-2103)

This mix was done at the KDOT Materials and Research Center Lab on September 29, 2021, by the KDOT Research Team. The team used the pre-weighed material constituents provided by KU and followed the mixing procedure provided by KU to mix the UHPC. The batch weights used are shown in the table below.

Table 1-2: Batch Weights Used in UHPC Mix

Material Type	Material Name	Batch Weight (lbs)
Cement	Monarch Type I	30.29
Silica Fume	Norchem SF	6.08
River Sand	Midwest Concrete Material (Perry, KS)	42.44
Fiber	Nycon Type I	5.88
Water	--	6.92
Superplasticizer	Euclid Plastol 6200 EXT	248.28 mL

The following tables summarize the fresh tests conducted and the samples made by KDOT.

Table 1-3: Fresh Property Tests Conducted

Test	Time of Testing (after mixing)
Temperature	0 min, 15 min, 30 min
Flow (ASTM C 1865)	0 min, 15 min, 30 min
Spread (ASTM C 1611)	0 min, 15 min, 30 min

Table 1-4: UHPC Samples Made by KDOT

Test	Day of Test	Sample Size	No. of Samples Made
Rapid Chloride Permeability (AASHTO T 277)	90 d	4”x8” cylinder	3
Surface Resistivity (KT-79)	Varies	4”x8” cylinder	Used RCP cylinders
Compressive Strength (ASTM C 1856)	Varies	3”x6” cylinder	11
Drying Shrinkage (ASTM C 157)	Varies	3”x3”x11.25” beam	2
Temperature (iButton)	--	4”x8” cylinder	Used one RCP cylinder
		Total No. of Samples =	**14 cyls, 2 beams**

2. OVERVIEW OF KDOT RESULTS

2.1 UHPC Mix at KU – 5/19/2021

The following table summarizes the results of KDOT's testing.

Table 2-1: Permeability Results

Time of Test	Volume of Permeable Voids (%)	Rapid Chloride Permeability (Coulombs)	Surface Resistivity (kΩ-cm)
28 d	3.9	--	39.7
56 d	--	463	--

Table 2-2: Freeze-Thaw Results

ID	Mix No.	Cut/Uncut?	No. of Cycles	Dynamic Modulus
UHPC	3751	Cut	720	99%
UHPC	3752	Uncut	720	99%

Table 2-3: Hardened Air Results

Sample No.	Hardened Air (%)	Spacing Factor (in)	Specific Surface (in^2/in^3)
1	2.79	0.0100	841.2
2	4.22	0.0102	693.3
3	4.68	0.0144	468.5

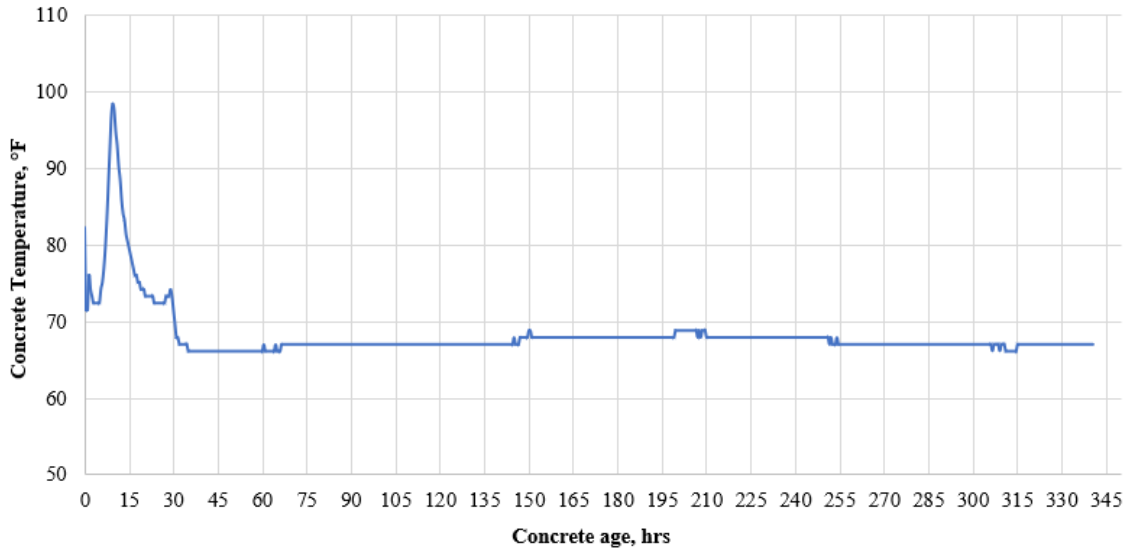

Figure 1 – Temperature data for UHPC mix.

Peak hydration temperature of 98.6 °F was reached at 9.5 hours.

2.2 UHPC Mix at KDOT MRC – 9/29/2021 (MRC# 21-2103)

The following table summarizes the results of KDOT's testing.

Table 2-4: Fresh Property Results

Time After Mixing	Concrete Temperature (°F)	Flow (C 1856) (in)	Spread (C 1611) (in)
0 min	89.1	5.375	17.125
15 min	85.3	5.2	16.375
30 min	82.2	5.125	16.75

Table 2-5: Hardened Property Results

Time of Test	Rapid Chloride Permeability (Coulombs)	Surface Resistivity (kΩ-cm)	Compressive Strength (ksi)
1 day	--	3.6	11.96
2 day	--	4.8	12.09
5 day	--	9.3	12.48
7 day	--	12.2	15.67
14 day	--	28.7	--
28 day	--	65.1	17.17
56 day	--	117.5	--
90 day	195	137.3	--

Table 2-6: Shrinkage Results

Day of Measure (Age)	ΔLx (%)	Std. Dev. (%)
Day 1	0.000	0.000
Day 5	-0.035	0.0021
Day 8	-0.044	0.0007
Day 15	-0.053	0.0014
Day 29	-0.063	0.0021
Day 292	-0.073	0.0007

Temperature/Maturity data for this mix is unavailable due to malfunction of the i-button temperature logging device.

AD ASTRA PER ASPERA

Kansas

Department of Transportation